**Contract No:**

This document was prepared in conjunction with work accomplished under Contract No. DE-AC09-08SR22470 with the U.S. Department of Energy (DOE) Office of Environmental Management (EM).

**Disclaimer:**

Savannah River National Laboratory®

A U.S. DEPARTMENT OF ENERGY NATIONAL LABORATORY • SAVANNAH RIVER SITE • AIKEN, SC

# PORFLOW Modeling of Vadose Zone Flow and Transport for the E-Area Low Activity Waste Vault

**F. G. Smith, III**

February 2021

SRNL-STI-2021-00063, Revision 0

SRNL.DOE.GOV

**DISCLAIMER**



**Printed in the United States of America**

**Prepared for**
**U.S. Department of Energy**

SRNL-STI-2021-00063
Revision 0

**Keywords:** *LAWV, Concrete, Waste Disposal, ELLWF*

**Retention:** *Permanent*

# PORFLOW Modeling of Vadose Zone Flow and Transport for E-Area Low Activity Waste Vault

F. G. Smith, III

February 2021

Prepared for the U.S. Department of Energy under contract number DE-AC09-08SR22470.

OPERATED BY SAVANNAH RIVER NUCLEAR SOLUTIONS

# REVIEWS AND APPROVALS

**AUTHORS:**

______________________________________________________________________
F. G. Smith, III, Environmental Sciences, SRNL

**TECHNICAL REVIEW:**

______________________________________________________________________
M. B. Gorensek, Advanced Modeling, Simulation, and Analytics, SRNL

**APPROVAL:**

______________________________________________________________________
D. G. Jackson, Manager
Environmental Sciences, SRNL

______________________________________________________________________
B. D. Lee, Director
Environmental & Biological Sciences, SRNL

# EXECUTIVE SUMMARY

In support of the E-Area Performance Assessment, a two-dimensional model of water flow and radionuclide transport through the E-Area Low Activity Waste Vault (LAWV) and local vadose zone has been developed using the PORFLOW™ software. The purpose of the model is to calculate flux to the water table for radionuclides eluted from the LAWV during its operational life, the period of institutional control, and times following site closure. Results of model calculations will be used by a three-dimensional PORFLOW model of transport through the aquifer to determine radionuclide concentrations at a hypothetical 100 meter well and at the site boundary where contaminated groundwater could be accessed by members of the public following site closure.

Although newly developed, the model structure closely follows that used in the 2008 PA while incorporating a refined computational mesh, updated material properties for the vadose zone soil and vault concrete (Nichols and Butcher, 2019), revised infiltration rates (Dyer 2019), and new solid-liquid distribution coefficients (Kaplan, 2016). The model also addresses degradation of concrete hydraulic properties by blending soil and concrete water retention curves over a 500 year period. That is, the hydraulic properties of LAWV concrete start out as fresh concrete at the time of site closure and degrade to soil properties over a 500 year time period. This approach has not been used previously in E-Area PAs and is also being applied in modeling Intermediate Level Vault concrete for the new PA.

The model has been used to calculate water flow through the LAWV vadose zone and, on a trial basis, transport of a limited number of radionuclides from the waste region inside the LAWV to the water table. Figure ES-1 provides a view of the model and an example of water flow after the concrete has partially degraded. Figure dimensions are in centimeters. The red area in both figures is the waste disposal region within the vault. Green and blue regions below the vault are respectively the upper and lower vadose zones. Other colored areas in the figures indicate different soil and concrete regions. Figure ES-2 shows the model calculation of flux to the water table (mol/yr) for Np-237 and its one-year half-life decay chain (Np-237 → U-233 → Th-229). Th-229 flux is too low to show on the same linear scale used for Np-237 and U-233 in the first part of Figure ES-2. The Np-237 peak is very sharp occurring at the time of vault roof collapse when flow through the vault increases significantly.

Results from these initial trial runs are compared to calculations that were made for the 2008 PA LAWV analysis. In brief, a new PORFLOW model of flow and transport through the LAWV vadose zone has been developed and tested.

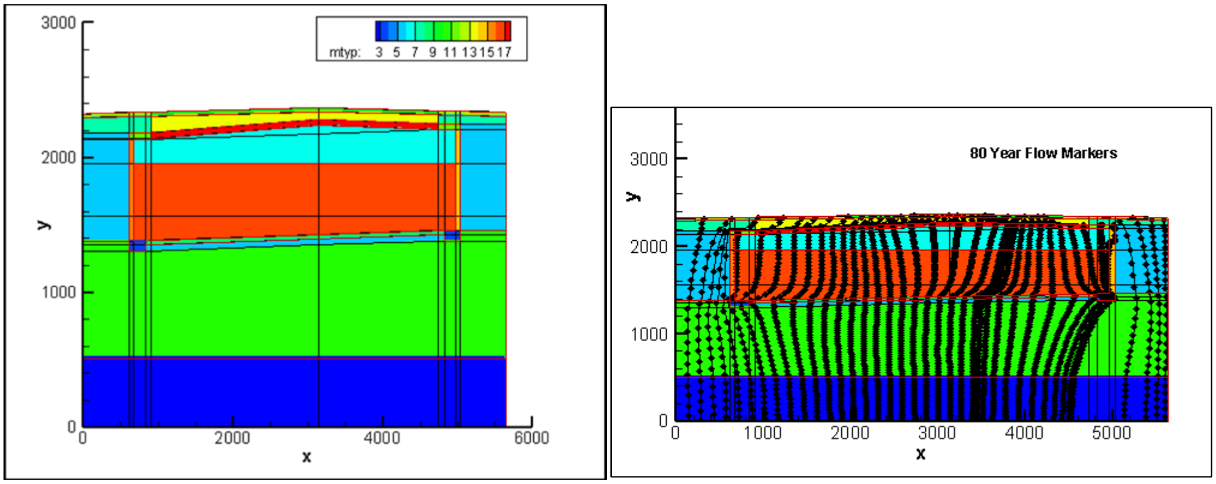


**Figure ES-1 LAWV Modeling Region and Water Flow 200 years After Site Closure.**

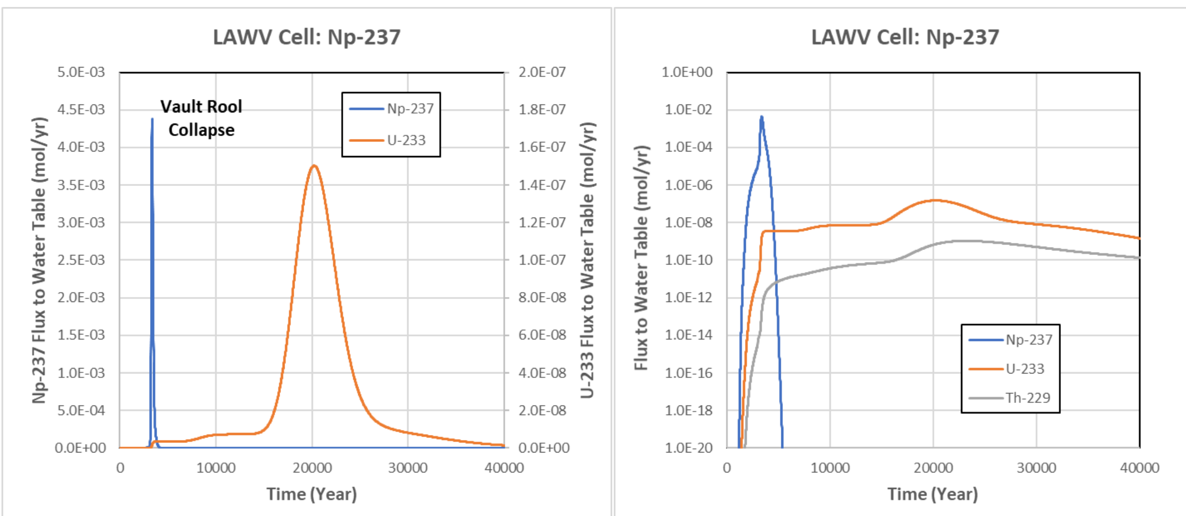


**Figure ES-2 Flux to water table for Np-237 and daughter radionuclides U-233 and Th-229.**

# TABLE OF CONTENTS

## LIST OF TABLES



## LIST OF FIGURES

## LIST OF ABBREVIATIONS

| | |
|---|---|
| AASHTO | American Association of State Highway and Transportation Officials |
| ELLWF | E-Area Low-Level Waste Facility |
| GCL | Geosynthetic Clay Layer |
| GSA | General Separations Areas |
| HDPE | High Density Polyethylene |
| HELP | Hydrologic Evaluation of Landfill Performance |
| IC | Institutional Control |
| ILV | Intermediate Level Vault |
| LAWV | Low Activity Waste Vault |
| LLW | Low Level Waste |
| LVZ | Lower Vadose Zone |
| OSC1 | Operational Soil Cover before dynamic compaction |
| PA | Performance Assessment |
| PAWG | Performance Assessment Working Group |
| UVZ | Upper Vadose Zone |

## 1.0 Introduction

The Low Activity Waste Vault (LAWV), usually referred to as the LAW Vault, is an above-grade reinforced concrete structure containing multiple layers of low-activity waste containers. The LAWV is used to dispose of waste containers exceeding radiological dose and radionuclide concentration limits of other, more cost effective, Low Level Waste (LLW) disposal facilities such as slit and engineered trenches but not requiring confinement in the Intermediate Level Vault (ILV). Figure 1-1 shows the location of the LAWV within the E-Area Low Level Waste Facility (ELLWF).

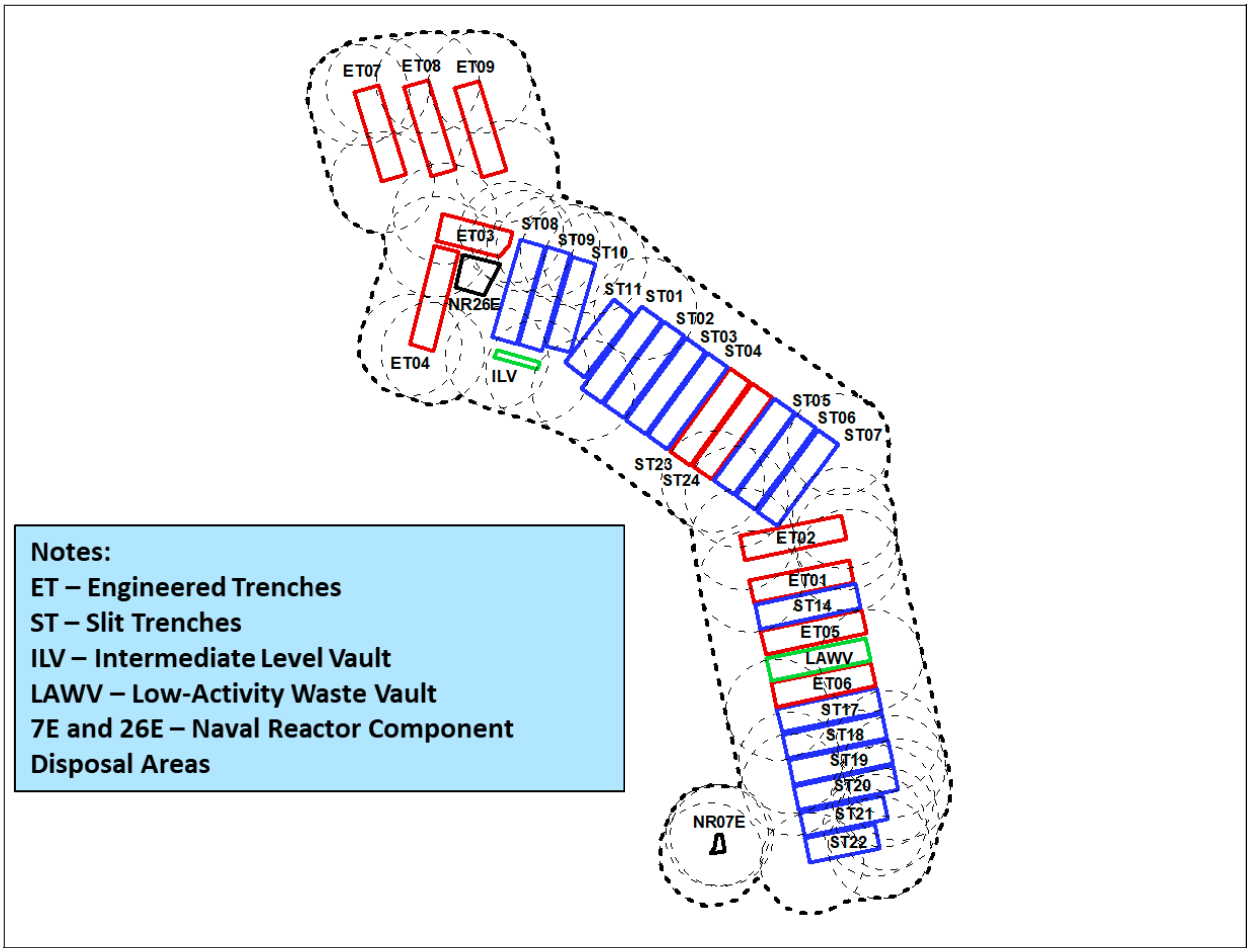


**Figure 1-1 Location of Low Activity Waste Vault within ELLWF.**

## 2.0 LAWV Background

The LAWV or LAW Vault is a large, above-grade, reinforced concrete structure approximately 643 feet (196 m) long, 145 feet (44.2 m) wide, and 27 feet (8.2 m) high at the roof crest. The LAWV is divided into 3 modules along its length, each of which are approximately 214 feet (65 m) long and contain 4 cells. The modules share a common footer but have a 2-inch gap between their adjacent walls. The 12 cell total is designed to contain more than 12,000 B-25 boxes of waste.

Figure 2-1 shows an aerial view of the LAWV exterior. The roof peak and slope can be just be made out in this view. Figure 2-2 shows an interior view of one cell with four levels of stacked B-25 waste containers in place. Figure 2-3 provides a simple plan view of the vault giving the overall dimensions, and Figure 2-4 shows a cross-sectional view (A-A') of a LAWV cell.

Figure 2-5 provides a schematic diagram depicting the two-dimensional PORFLOW ™ model of the LAWV. The diagram is not to scale and the full PORFLOW model includes the vadose zone below the vault, soil backfill around and over the vault, and the closure cap above the foundation layer. The model represents a slice through the vault cross-section. LAWV dimensions used to build the PORFLOW model were taken from Figure 2-4 and the two figures can be compared to discern modeling approximations. For example, the floor footing that extends beyond the vault walls was not included in the model because it would have little effect on flow and transport. Note that the height of the south wall is very close to that of the north wall but is not identical. The dimensions given in Figure 2-4 and specified slopes of the floor and roof were used to calculate model dimensions which resulted in the south wall being three inches taller than the north wall.

The following paragraphs describing LAWV operation and closure were extracted from the 2008 Performance Assessment (PA) (WSRC, 2008) where they are attributed to the following sources: McDowell-Boyer et al. 2000 and Cook et al. 2004.

During the 25-year operational period {*71 years is assumed to be the operational period in the 2022 PA*}, low-activity waste contained in metal boxes (predominately B-25 boxes and B-12 boxes), drums and/or concrete containers will be stacked by forklift within the LAWV. B-25 boxes (approximately 4-foot high by 6-foot long by 4-foot wide) and/or equivalent pairs of B-12 boxes (approximately 2-foot high by 6-foot long by 4-foot wide) are stacked four high. Waste within the containers typically includes job control waste, scrap metal, and contaminated soil and rubble. Job control waste consists of potentially contaminated protective clothing (plastic suits, shoe covers, lab coats, etc.), plastic sheeting, etc. The scrap metal consists of contaminated tools, process equipment and piping, and laboratory equipment. Soil and rubble are generated from demolition activities. The average waste density within the containers has been estimated to be 0.1785 g/cm$^3$ (Phifer and Wilhite 2001) which results in a large subsidence potential of approximately 21 feet (Jones and Phifer 2006).

Operational closure of the LAWV will be conducted in stages. Individual cells will be closed as they are filled with stacks of containerized waste (metal and/or concrete containers) and the entire vault will be closed after it is filled. {*In practice, cells have not been closed and some waste stored in the LAWV has been reclassified and transferred to trenches for final disposal. At present, only metal containers, primarily B-25 boxes, are disposed in the LAWV*} Operational closure includes filling the interior water collection trench and exterior sump with grout and sealing exterior vault openings, including those between modules, with reinforced concrete equivalent to that utilized in the vault floor, walls and roof. The reinforcing steel will be tied into the reinforcing steel of the vault itself, forming a unified structure with continuous walls. No additional closure actions are anticipated beyond that of operational closure for the LAWV during the 100-year institutional control period (i.e. interim closure).

Final closure of the LAWV will take place at final closure of the entire ELLWF, at the end of the 100-year institutional control period (Phifer 2004). Final closure will consist of the installation of an integrated closure system designed to minimize moisture contact with the waste and to provide an intruder deterrent. The integrated closure system will consist of a closure cap installed over all the disposal units and a drainage system. The apex of the closure cap will extend the length of the LAWV and be approximately centered over the vault in order to minimize the overburden loads on the vault and maximize runoff and lateral drainage from the overlying closure cap. {*In the 2022 PA a new conceptual closure cap design has the final closure cap sloping away from the LAWV roof peak in both directions along the long and short axis of the vault.*} After installation it is assumed that no closure cap maintenance will be performed other than that required for establishment of the vegetative cover. Therefore, it is assumed that the hydraulic properties of the closure cap will immediately begin to degrade after construction due to the following effects (Phifer and Nelson 2003; Phifer 2004):

- Formation of holes in the upper (Geosynthetic Clay Layer) GCL by pine forest succession. {*A high-density polyethylene (HDPE) geomembrane liner has been added above the geosynthetic clay layer in the most recent conceptual closure cap design. The geomembrane provides the primary barrier to water infiltration*.}
- Reduction in the saturated hydraulic conductivity of the drainage layers due to colloidal clay migration into the layers.
- Erosion of layers that provide water storage for the promotion of evapotranspiration.

Table 2-1 provides a summary of significant features of the LAWV construction along with a brief description of the modeling approach used.

**Table 2-1 LAWV Construction Features and Modeling Approach**

| As Built LAWV Features | As Modeled |
|---|---|
| Controlled compacted backfill soil base | LAWV soil base modeled as upper vadose zone soil. Thickness of compacted backfill was not provided. |
| Crusher run stone base over a geotextile filter fabric beneath the vault. | Area beneath the vault modeled as upper vadose zone soil. Crusher run stone base would silt-up following closure. |
| 1.25-foot graded stone sub-drainage system to collect and drain any water under the vault to manhole drains during operations. Sealed with grout at end of operations. | Water under the vault conservatively drains to the water table. Sub-drainage system is sealed, grouted and is not functional after the end of operations. |
| 2.5-foot-thick, reinforced concrete, wall supports which extend 4.5 feet beyond the exterior walls. | Concrete wall supports are modeled without the 4.5-foot extensions beyond the exterior walls. |
| 1-foot thick, cast-in-place, reinforced concrete floor slab sloped to an interior collection trench, which drains to an external sump. | Sloped concrete floor modeled without drainage to external sump to conserve water and maintain material balances around the model. Sump will be grouted at end of operations. |
| Exterior and interior personnel openings with doors, exterior fan openings, and exterior forklift access openings during operations. Sealed with reinforced concrete at the end of operations | Cell walls modeled as continuous E-Area vault concrete structures. |
| AASHTO Type IV bridge beams to support the concrete roof. | Vault interior construction is not modeled. Vault space above the waste region is modeled with waste material properties to allow good water drainage into the waste zone. No radionuclides are deposited in this region |
| 3-½ inch thick precast deck panels overlain by 12-½ inch thick cast-in-place, reinforced concrete slab for a total 16-inch thick concrete roof. | Roof modeled as continuous 16-inch thick E-Area vault concrete. |
| A bonded-in-place layer of fiberboard insulation and a layer of waterproof membrane roofing on top of the roof slab | Sloped concrete roof is assumed to be in place from the start of LAWV operations until roof collapse occurs. The presence of fiberboard insulation and waterproofing on the roof top is simulated by using a very low infiltration rate (0.001 inch/year) over the vault during operation and institutional control. |
| A gutter/downspout system to drain the roof | Water draining off the roof is not included in lateral flow to water table during operations and institutional control. Gutters and downspouts will be removed when final closure cap is installed. |

## 2.1 LAW Vault Structural Stability and Cover Integrity

The LAWV is designed to withstand Design Basis Accident loads that ensure continued structural stability during its anticipated life. Carey (2005) conducted a structural degradation prediction analysis and documented the significant degradation points in the life of the LAWV. These are listed below along with the modeling used to simulate the event. Years given are time from placement of the final closure cap.

- Upon placement of the closure cap overburden, non-through-slab static cracking of the LAWV roof slab will occur and remain relatively constant over time.
  - Modeling: When the closure cap is placed, roof and roof beam concrete hydraulic properties change from 100% E-Area Concrete to a blend of 90% E-Area Concrete and 10% gravel.
- Upon placement of the closure cap overburden, non-through-wall static cracking of the LAWV exterior side walls will occur and increase slightly over time.
  - Modeling: When the closure cap is placed, wall concrete hydraulic properties change from 100% E-Area Concrete to a blend of 90% E-Area Concrete and 10% gravel.
- The LAWV roof slab will collapse due to closure cap loading, seismic loading, and rebar corrosion at a mean time of 2805 years with a standard deviation of 920 years.
  - Modeling: The LAWV roof acquires the hydraulic properties of soil 500 years after the closure cap is placed and transport properties of soil 2805 years after the cap is placed. Infiltration over the vault is increased at 2805 years to simulate both the absence of a closure cap and collection of roof runoff in the collapsed region.
- The LAWV exterior side walls will collapse due to closure cap loading, seismic loading, and rebar corrosion at a mean time of 9415 years with a standard deviation of 2290 years.
  - Modeling: Conservatively, all LAWV concrete acquires the hydraulic properties of soil 500 years after cap placement and transport properties of soil when the roof collapses.
- Differential settlement due to seismic loading could result in through-wall cracking of the side walls that opens into the roof slab with a probability of 0.8% over a 1000 year period.
  - Modeling: Low probability event is not included in the modeling. However, concrete properties degrade to those of soil within 500 years.
- Differential settlement due to seismic loading could result in through-wall cracking of the side walls that opens into the footer with a probability of 1.2% over a 1000 year period.
  - Modeling: Low probability event is not included in the modeling. However, concrete properties degrade to those of soil within 500 years.
- Within 50 to 100 years after placement of the closure cap overburden, differential settlement between the wall footers and floor slab will occur due to differences in static loading between the two resulting in a separation between the footers and floor slab.
  - Modeling: When the closure cap is placed, wall footer concrete hydraulic properties change from 100% E-Area Concrete to a blend of 90% E-Area Concrete with 10% gravel. As explained in Section 5.3, hydraulic performance of the footer concrete, like the roof and walls, degrades over a 500 year period by blending with the hydraulic properties of soil increasing the soil content in 10% increments every 50 years. The

floor degrades in a similar fashion but does not include 10% gravel. This means that the wall footers provide a preferential flow path during the period of concrete degradation thereby simulating separation between the footer and the floor.

- Differential settlement beneath the floor slab due to seismic loading could result in flexural cracking of the floor slab. The probability of such an event occurring over a 1000 year period has been estimated to be 50%.
  - Modeling: Hydraulic properties of floor concrete degrade from concrete to soil properties over a 500 year period following closure cap placement.

The waste subsidence potential of 21 feet does not impact the structural stability of the LAW Vault until the time of anticipated, roof structural failure at 2805 years. At the time of roof failure, it is assumed that the LAWV roof will collapse into the vault itself and that subsidence of the waste will occur. After roof collapse, the GCL drainage layer in the closure cap (Section 5.1) is given the properties of backfill soil.

**Figure 2-1 Aerial view of LAWV.**


**Figure 2-2 Interior View of LAWV Cell.**

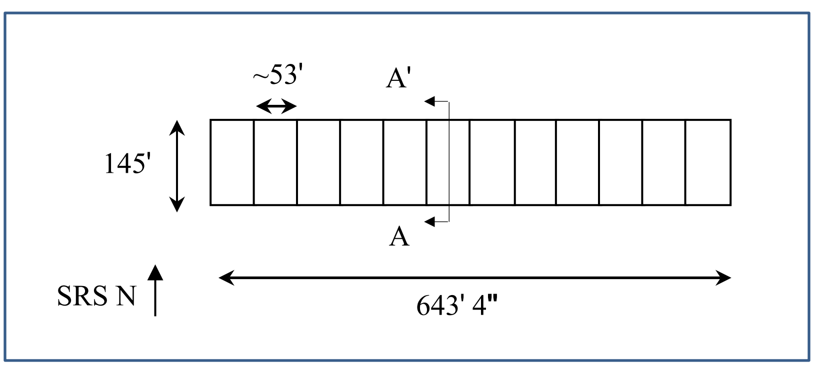


**Figure 2-3 Simple plan view of LAWV.**

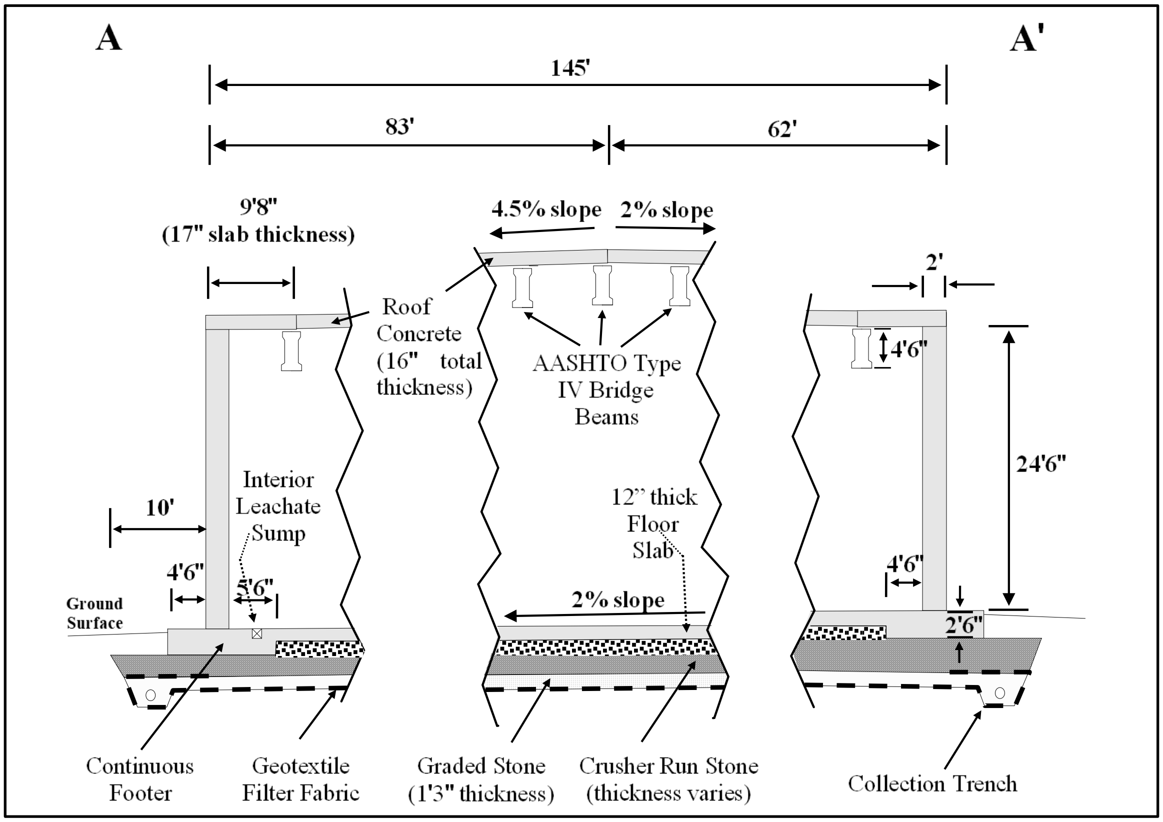


**Figure 2-4 Cross-sectional view of LAWV.**

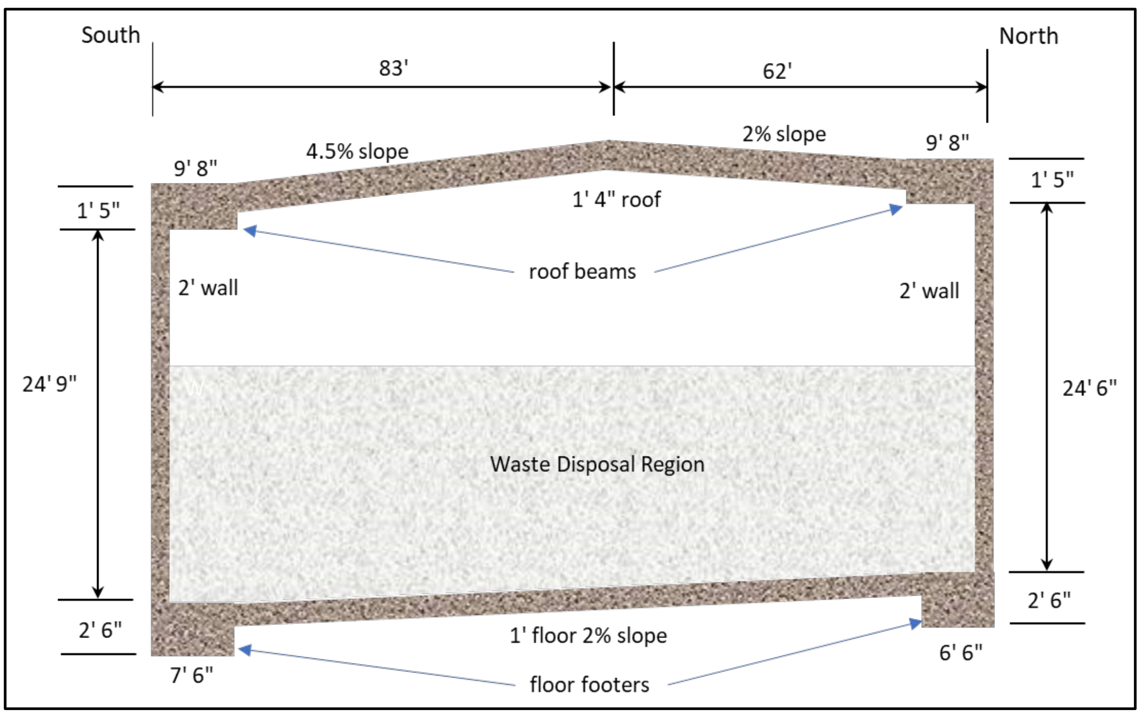


**Figure 2-5 Schematic representation of PORFLOW model of LAWV.**

## 3.0 LAWV Timeline

Table 3-1 provides an overview of the LAWV timeline assumed in developing the PORFLOW model. Model timing (time = 0) starts with the receipt of the first disposal container in the LAWV in late 1994. As a conservative approach, flow and transport modeling assume the entire waste inventory is placed at the start of operations. This allows daughter ingrowth to occur for decay chains and does not significantly reduce the concentration of long-lived radionuclides such as C-14, Tc-99 and I-129, which are typically strong contributors to dose. Radionuclides with very short half-lives such as tritium will largely decay away prior to the 1000-year post-closure period during which the performance of the LAWV is assessed for regulatory compliance and the assumption of early disposal is acceptable.

As described in Section 4.3, hydraulic properties of the vault concrete are assumed to degrade over a 500-year period starting at the end of institutional control when moisture buildup in the overlying cap, vault cracking and lack of access to the subdrain system lead to water infiltration through the vault. Based on the structural analysis performed for the LAWV (Carey, 2005), installation of the final closure cap results in cracking that partially penetrates the vault walls and roof causing some immediate degradation in concrete hydraulic properties. The structural analysis also concluded that the vault roof would collapse from a combination of degradation and seismic events at a mean time of 2805 years after installation of the closure cap.

**Table 3-1 LAWV Timeline**

| Calendar Date | Numerical Calendar Date | Time from Start of LAWV Operation | Operational Events |
|---|---|---|---|
| 9/28/1994 | 1994.74 | 0.0 | Start of ELLWF operations.<br>Start of LAWV operations.[1]<br>Start radionuclide decay and daughter ingrowth in waste material.<br>Start 10,000-year modeling period. |
| 9/28/2065 | 2065.74 | 71.0 | End of ELLWF operations.<br>End of LAWV operations<br>Start of institutional control. |
| 9/28/2165 | 2165.74 | 171.0 | End of institutional control.<br>Installation of final closure cap.<br>Non-through cracking of vault roof, roof beams, walls, and wall footers.[2]<br>Start 500-year concrete degradation.<br>Start 1000-year compliance period. |
| 9/28/2215 | 2215.74 | 221.0 | Separation between wall footers and floor slab from differential settlement.[3] |
| 9/28/2665 | 2665.74 | 671.0 | Vault concrete fully degraded assuming the hydraulic properties of uncompacted operational soil cover (OSC1). |
| 9/28/3165 | 3165.74 | 1171.0 | End of 1000-year compliance period.<br>Additional floor cracking from differential settlement. |
| 9/28/4970 | 4970.74 | 2976.0 | Vault roof collapse. Waste material subsides from initial 21.8 ft layer into 4.5 ft layer at bottom of vault.[4] Waste and vault concrete assume transport properties of clayey soil. |
| 9/28/5156 | 5165.74 | 3171.0 | Side wall through cracking occurs which opens into roof and wall footers.[5] |
| 9/28/11580 | 11,580.74 | 9586.0 | Side walls collapse.[5] |
| 9/28/12165 | 12,165.74 | 10,171.0 | End of 10,000-year post-institutional control modeling period.[6] |

[1]Conservativly, it is assumed that all the waste in the LAWV is placed at the start of operations.
[2]The structural analysis predicts that roof cracking remains constant and wall cracking increases slightly over time.
[3]Separation predicted to occur between 50 and 100 years after closure cap is placed
[4]Waste depths are measured under the roof peak.
[5]These events occur well beyond the period of compliance and were not included in the modeling. All vault concrete is assumed to have the flow properties of soil at 671 years and the transport properties of soil at 2976 years.
[6]For some radionuclides, modeling will be extended to 50,000 years to capture peak radionuclide concentrations.

## 4.0 LAWV Vadose Zone Hydro-stratigraphic Layers

Figure 4-1 shows a generalized (not to scale) one-dimensional schematic diagram of the LAWV disposal site and the underlying vadose zone hydro-stratigraphic layers. The diagram is only intended to show the vadose zone layers and omits many details of the actual PORFLOW model (see Figure 2-5). Dimensions of the zones for the LAWV disposal site (Bagwell and Bennett, 2018) and specification of soil material in the model are listed in Table 4-1. At the LAWV site, the water table is above the tan clay confining zone.

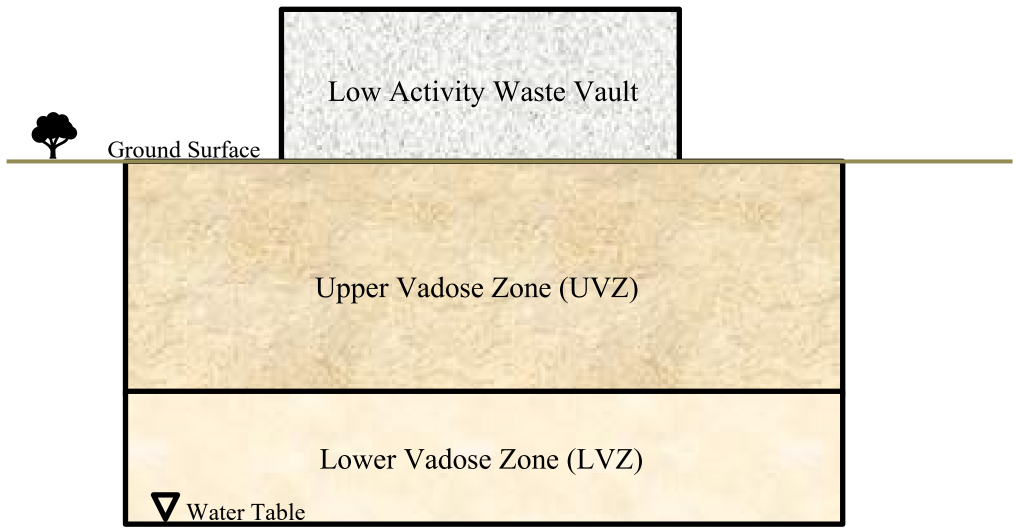


**Figure 4-1 Schematic representation of LAWV waste disposal site and vadose zone hydro-stratigraphic layers.**

**Table 4-1 Nominal Thickness in Feet and Composition of LAWV Vadose Zone Segments**

| Vadose Zone Segments | Segment Length (feet) |
|---|---|
| Average Depth to Water Table | 46.8 feet |
| UVZ | 30.1 feet Clay |
| LVZ | 16.7 feet Sand |

# 5.0 Model Description

## 5.1 LAWV Model Geometry

Figure 5-1 provides a cross-sectional view of the LAWV with the final closure cap in place taken from design document C-CT-E-00084. As shown in Figure 1-1, the LAWV site is located between Engineered Trenches 5 and 6 within the ELLWF. Therefore, because the LAWV creates a high point in the area, the final closure cap slopes away from the LAWV roof peak in both directions. As discussed in Section 5.2 below, infiltration rates calculated to pass through the High-Density Polyethylene (HDPE) geomembrane which lies just above the Geosynthetic Clay Layer (GCL) are used as an upper boundary condition in the PORFLOW model. The geomembrane is the limiting barrier to infiltration in the closure cap design. The PORFLOW model includes the GCL and the soil layer placed over the vault (referred to as the "foundation layer" in Figure 5-1). The GCL has a higher hydraulic conductivity than the foundation soil and functions as a drainage layer channeling some of the infiltration water that passes through the geomembrane away from the LAWV.

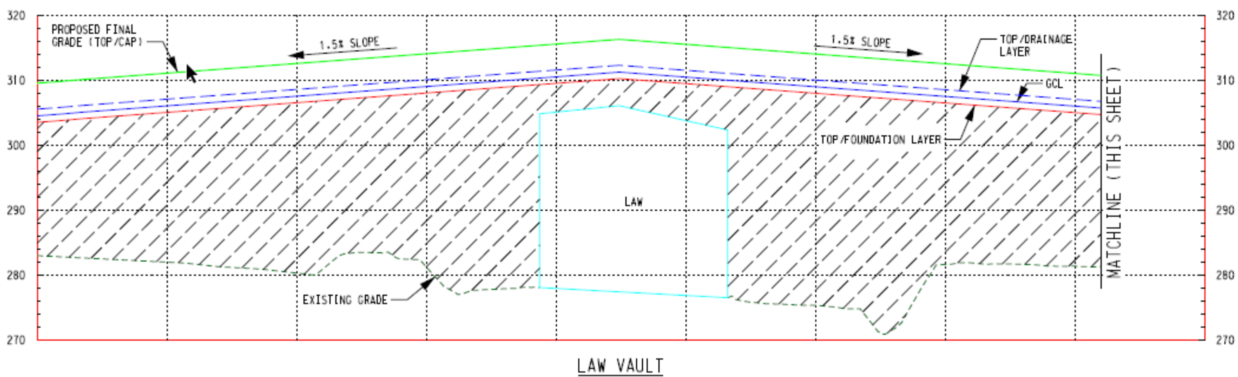


**Figure 5-1 Detail of LAWV Final Closure Cap Configuration (C-CT-E-00084, 2016).**

Figure 5-2 shows the PORFLOW model geometry with different material types color coded. Figure 5-2 is oriented south to the right and north to the left which is opposite to Figure 5-1. To give some perspective, the waste region in the vault is red and the void region above the waste is white. Upper Vadose Zone (UVZ) and Lower Vadose Zone (LVZ) are marked in the figure and soil backfill is the light blue region on either side of the vault.

In Figure 5-2 horizontal and vertical dimensions are in centimeters. Therefore, the 5638.8 cm horizontal model dimension represents a model domain 185 feet long. The LAW Vault cross-section is 145 feet (4419.6 cm) wide with the computational grid extending 20 feet (609.6 cm) to the north and south of the vault. The additional 20 feet includes an area under the closure cap to account for drainage away from the vault and possible flow into the vadose zone beneath the LAWV from background infiltration and roof runoff. As shown in Figure 1-1, the LAWV lies between two engineered trenches. This restricted the side soil widths to 20 feet to avoid vadose zone regions that might be affected by the presence of the trenches. From its peak, the LAWV roof slopes 2% to the north and 4.5% to the south. The closure cap slopes 1.5% away from the LAWV roof peak in both directions.

Figure 5-3 shows a close-in view of the computational mesh immediately around the upper north corner of the LAWV. This figure gives an indication of the mesh detail and provides a better view of the vault concrete, closure cap, and the surrounding soil. Because parts of the vault concrete are modeled with different properties, they are identified as different materials. Material properties were obtained from the latest property database (Nichols and Butcher, 2020).

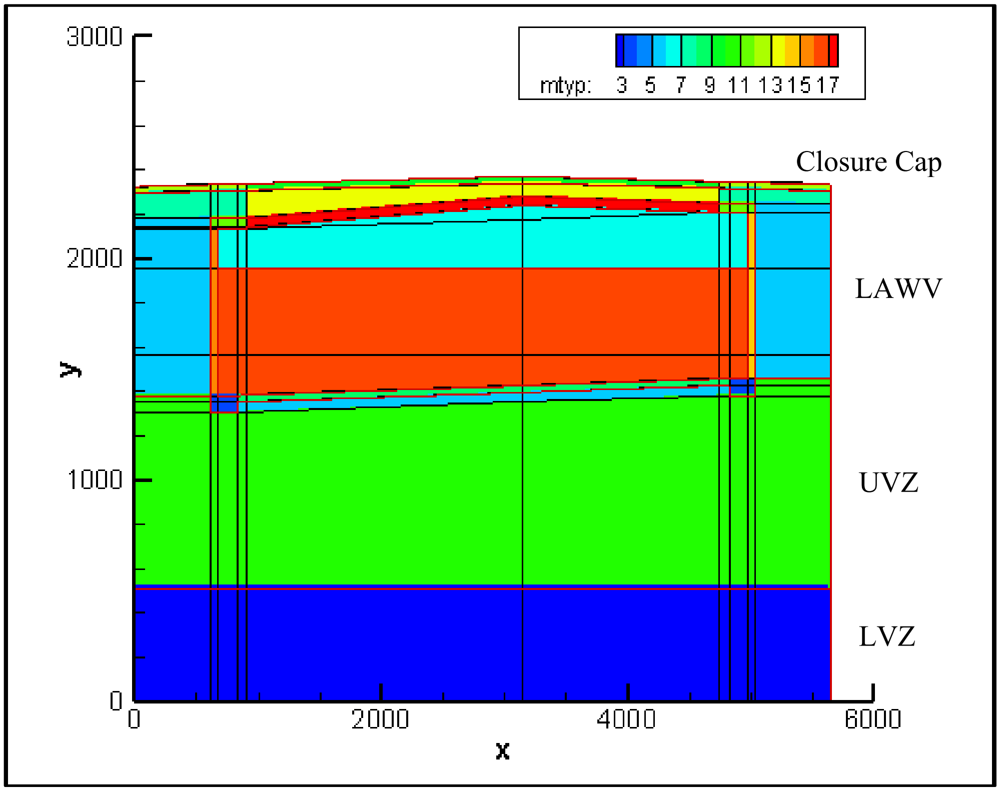


**Figure 5-2 PORFLOW Model of LAWV Cell and Vadose Zone.**

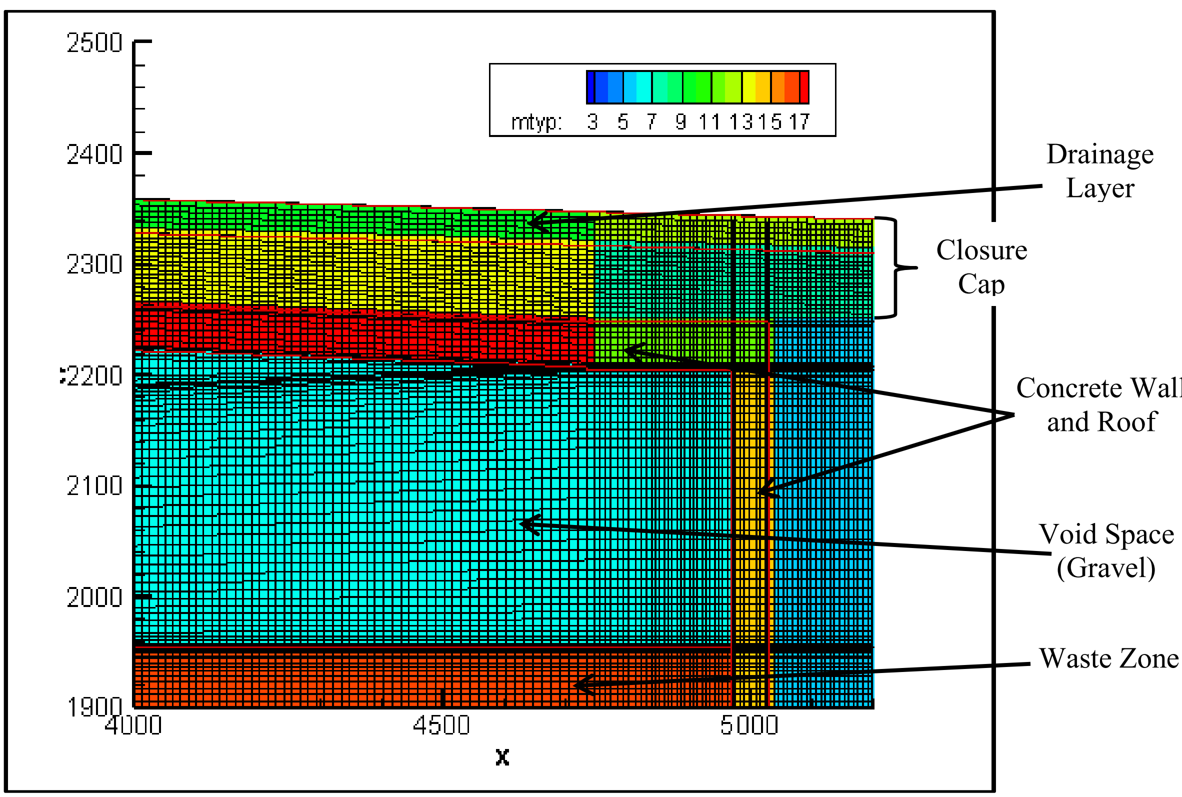


**Figure 5-3 Portion of Computational Mesh in LAWV Model.**

## 5.2 Infiltration Boundary Conditions

Infiltration rates through the LAWV and surrounding area applied in the PORFLOW model are listed in Table 5-1. In this table, the abbreviation IC stands for Institutional Control. On-Vault is infiltration directly over the vault and Off-Vault is infiltration over the 20 ft side regions.

The concrete vault roof in place during operations can be seen in Figure 2-1. As shown in Figure 2-4 and Figure 2-5, the roof slopes 2.5% to the north side and 4.5% to the south side. The roof has an overlying bonded-in-place fiberboard insulation and a waterproof membrane that effectively prevents rainwater from entering the cells. This sloped roof with overlying waterproof membrane will remain uncovered during the 71 year E-Area operational period (1994-2065) and the following 100-years of institutional control (2065-2165). There will essentially be no water infiltration into the vault during this time for the following reasons:

- A roof slope of 2% to the north and 4.5% to the south along with the overlying waterproof membrane will shed rainwater from the top of the vault to gutters and downspouts that collect the water.
- The initial intact condition of the LAWV roof and guttering will be maintained during E-Area operations and the 100 year period of institutional control.
- Absence of a soil cover during operations and institutional control prevents buildup of soil moisture above the roof. The PORFLOW model always includes the soil cover. However, for modeling purposes, a small infiltration rate of 0.001 in/yr is assumed to apply over the vault for the first 171 years of the simulation.

At the end of institutional control, the final closure cap will be placed over the entire ELLWF. Infiltration rates above the LAWV and the surrounding soil cover from the time of final closure cap placement to 2905 years beyond, when it was predicted that the vault roof collapses, have been calculated using the Hydrologic Evaluation of Landfill Performance (HELP) model (Dyer, 2019). Beyond 2905 years infiltration rates are assumed to remain constant. A structural analysis of the LAWV (Carey, 2005) determined the mean time to roof collapse from a combination of load stresses from the closure cap, seismic events and rebar corrosion.

During the first 500 years following the end of institutional control, the model degrades concrete hydraulic properties and at 500 years assumes that hydraulically the concrete behaves like soil (concrete transport properties are retained until roof collapse). The model adjusts concrete properties in 50-year time steps by blending hydraulic properties for concrete with those of the operational soil cover. A description of the process for blending the hydraulic properties of concrete with soil is provided below in Section 5.3. Because these time steps did not coincide with the HELP model infiltration calculations, the HELP results were linearly interpolated to follow the 50-year incremental changes in material properties.

Subsequently, it was decided to smooth HELP infiltration predictions over 34 time periods using linear interpolation. The additional flow solutions serve to smooth out results from the radionuclide transport calculations. Results of this interpolation are shown in Table 5-1 where the shaded area from 171 to 671 years is the 500 years when concrete degradation occurs. The column "HELP Times" gives the HELP infiltration times used to make the interpolation. PORFLOW preprocessing also averages infiltration rates over the time steps. For example, if the HELP infiltration rate at time T(i) is I(i) and at time T(i+1) is I(i+1), PORFLOW will use infiltration rate 0.5*[I(i) + I(i+1)] for flow time period T(i) to T(i+1). Infiltration rates in Table 5-1 are averaged values to show exactly what the PORFLOW model is using. PORFLOW calculates 34 steady-state flow solutions over the entire computational domain using the infiltration rates as a boundary condition on the top surface. These flow solutions are then used to make the radionuclide transport calculations.

Figure 5-4 plots the 34 infiltration rates showing the associated time intervals. Table 5-1 also shows that, once the final closure cap is in place, infiltration over the vault ("On-Vault" infiltration) and the 20-foot capped regions on either side of the vault ("Off-Vault" infiltration), are identical until the vault roof collapses at 2976 years. Following roof collapse, flow through the vault is higher than background because it is collecting runoff from the upslope portion of the intact closure cap. Off-Vault infiltration to the areas beside the vault are only different before the closure cap is placed and after roof collapse.

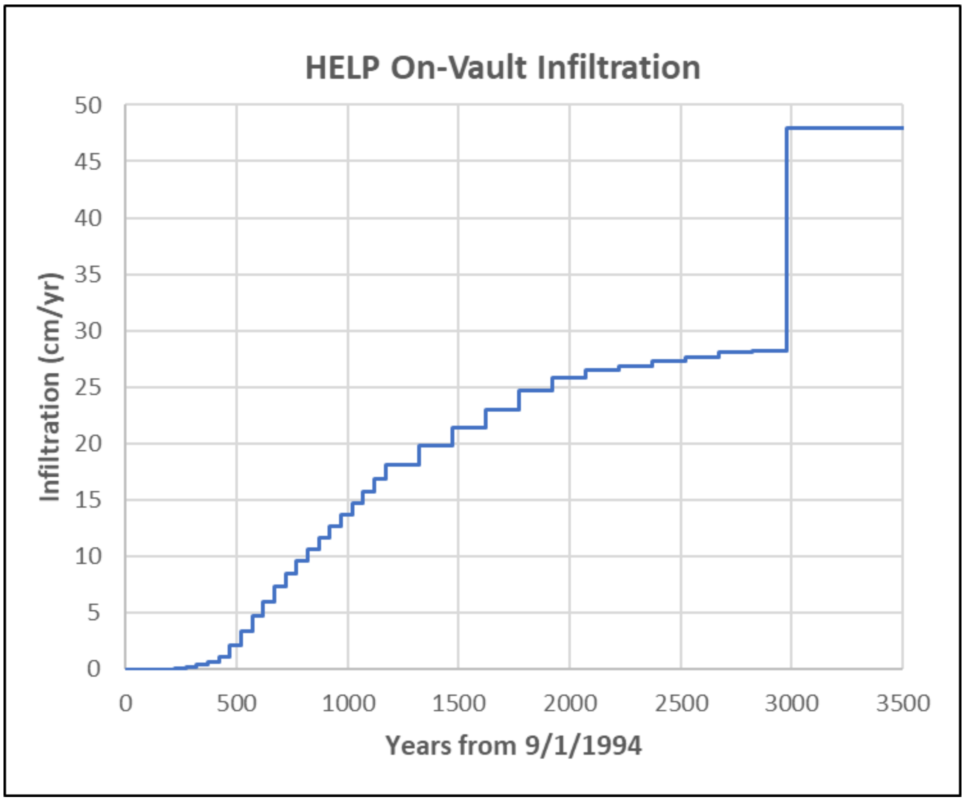


**Figure 5-4 Interpolation of HELP On-Vault Infiltration to PORFLOW Time Zones.**

**Table 5-1 LAWV Infiltration Rates**

| | Numerical Calendar Date | HELP Times[1] (Year) | Start Time (Year) | LAWV Event | Infiltration (cm/year) | |
|---|---|---|---|---|---|---|
| | | | | | On-Vault | Off-Vault |
| 1 | 1994.74 | | 0 | Start of ELLWF and LAWV Operations | 0.0012 | 40.081 |
| | 2065.74 | 0 | 71 | Start of IC | | |
| 2 | 2165.74 | 100 | 171 | End of IC Closure Cap Placed Start Compliance Period | 0.007 | |
| 3 | 500 Year Period of Concrete Degradation (From Year 171 to Year 671) | 100 - 180 | 221 | | 0.050 | |
| 4 | | 180 - 290 | 271 | | 0.177 | |
| 5 | | | 321 | | 0.361 | |
| 6 | | 300 | 371 | | 0.635 | |
| 7 | | 340 - 380 | 421 | | 1.146 | |
| 8 | | 380 - 480 | 471 | | 2.120 | |
| 9 | | | 521 | | 3.405 | |
| 10 | | 480 - 660 | 571 | | 4.699 | |
| 11 | | | 621 | | 5.997 | |
| 12 | | | 671 | Vault Hydraulic Failure | 7.295 | |
| 13 | 2715.74 | 480 - 660 | 721 | | 8.489 | |
| 14 | 2765.74 | 660 - 1100 | 771 | | 9.551 | |
| 15 | 2815.74 | | 821 | | 10.587 | |
| 16 | 2865.74 | | 871 | | 11.624 | |
| 17 | 2915.74 | | 921 | | 12.660 | |
| 18 | 2965.74 | | 971 | | 13.696 | |
| 19 | 3015.74 | | 1021 | | 14.732 | |
| 20 | 3065.74 | | 1071 | | 15.768 | |
| 21 | 3115.74 | | 1121 | | 16.805 | |
| 22 | 3165.74 | 1100 | 1171 | End Compliance Period | 18.137 | |
| 23 | 3315.74 | 1100 - 1900 | 1321 | | 19.766 | |
| 24 | 3465.74 | | 1471 | | 21.395 | |
| 25 | 3615.74 | | 1621 | | 23.024 | |
| 26 | 3765.74 | | 1771 | | 24.652 | |
| 27 | 3915.74 | | 1921 | | 25.871 | |
| 28 | 4065.74 | 1900 - 2723 | 2071 | | 26.474 | |
| 29 | 4215.74 | | 2221 | | 26.872 | |
| 30 | 4365.74 | | 2371 | | 27.270 | |
| 31 | 4515.74 | | 2521 | | 27.668 | |
| 32 | 4665.74 | | 2671 | | 28.036 | |
| 33 | 4815.74 | 2723 - 2905 | 2821 | | 28.238 | |
| 34 | 4970.74 | 2905 | 2976 | Roof Collapse | 47.981 | 28.219 |
| | >4970.74 | >2905 | 10,170 | End Simulation | 47.981 | 28.219 |

[1]HELP times show the times used for interpolation. For example, HELP infiltrations calculated at 660 years and 1100 years were used to interpolate infiltration rates for time steps 14 – 21.

### 5.3 Modeling Concrete Degradation

In past PAs, the hydraulic properties of concrete have been abruptly changed from those of intact concrete to soil to represent vault structural collapse or complete deterioration of the concrete matrix. In this PA, concrete degradation is modeled as a gradual process where, starting at the time of site closure, concrete hydraulic properties are transformed into those of soil over a period of 500 years. The 500-year post closure end point is adopted from the PA Working Group (PAWG) recommendation in NUREG-1573. An excerpt from this document (¶2 Section 3.2 "Performance of Engineered Barriers") is reproduced below:

> However, to limit unnecessary speculation as to their performance, the PAWG believes that materials typically used in engineered barriers can alternatively be assumed to have physically degraded after 500 years following site closure. Thus, at 500 years and beyond, the engineered barriers can be assumed to function at levels of performance that are considerably less than their optimum level, but credit for structural stability and chemical buffering effects may be taken for longer periods of time.[1] For timeframes longer than 500 years, it is unreasonable to assume that any physical engineered barrier such as a cover or a reinforced concrete vault can be designed to function long enough to influence the eventual release of long-lived radionuclides such as carbon-14 (half-life: 5300 years); technetium-99 (half-life: 213,000 years); and iodine-129 (half-life: 15,700,000 years), if they are present. However, credit for structural stability and chemical buffering effects may be taken for the long-term provided that the applicant provides suitable information and justification. But again, this would have to be evaluated on a case-by-case basis.

Based on this recommendation, the LAWV and ILV models use a blend of concrete and soil to determine hydraulic properties in 50-year increments over the assumed 500-year lifetime of E-Area Vault concrete. At site closure, structural analysis of the LAWV (Carey, 2005) predicts that the LAWV roof and walls will experience limited non-through static cracking when the final closure cap is placed over the vault. Upon final closure, initial hydraulic properties for concrete in the vault roof, roof beams, walls, and wall footers are calculated as a blend of 90% E-Area Vault Concrete and 10% Gravel to represent the impact of early stress cracking in the concrete. Soil being blended with the concrete is represented by the hydraulic properties of operational soil cover before dynamic compaction (OSC1). Table 5-2 provides a list of the material blends used to represent concrete degradation following site closure and the saturated hydraulic conductivity of each blend. The model further assumes that concrete sorption properties adjusted for aging effects, are maintained until roof collapse.

**Table 5-2 LAWV Material Blends for Degraded Concrete**

| Years Post Closure | Roof, Roof Beams, Walls and Wall Footers | | | Floor | | |
|---|---|---|---|---|---|---|
| | 90% Concrete 10% Gravel[1] | Soil | $K_{sat}$ (cm/s) | E-Area Concrete | Soil | $K_{sat}$ (cm/s) |
| 0 | 100% | 0% | 1.80E-11 | 100% | 0% | 1.00E-12 |
| 50 | 90% | 10% | 9.84E-11 | 90% | 10% | 7.64E-12 |
| 100 | 80% | 20% | 5.21E-10 | 80% | 20% | 5.61E-11 |
| 150 | 70% | 30% | 2.69E-09 | 70% | 30% | 3.96E-10 |
| 200 | 60% | 40% | 1.35E-08 | 60% | 40% | 2.69E-09 |
| 250 | 50% | 50% | 6.61E-08 | 50% | 50% | 1.76E-08 |
| 300 | 40% | 60% | 3.16E-07 | 40% | 60% | 1.12E-07 |
| 350 | 30% | 70% | 1.47E-06 | 30% | 70% | 6.84E-07 |
| 400 | 20% | 80% | 6.70E-06 | 20% | 80% | 4.05E-06 |
| 450 | 10% | 90% | 2.98E-05 | 10% | 90% | 2.33E-05 |
| 500 | 0% | 100% | 1.30E-04 | 0% | 100% | 1.30E-04 |

[1]Gravel $K_{sat}$ = 1.50E-01 cm/s

*5.3.1 Property Blending*

Hydraulic properties for a mixture of concrete and another material (in this case soil or gravel) are typically calculated as described by Flach (2017). Composite porosity ($\epsilon_b$) and saturated hydraulic conductivity ($K_b$) are calculated from the equations:

$$\epsilon_b{}^p = f_c\,\epsilon_c{}^p + f_s\,\epsilon_s{}^p \quad (1)$$

$$K_b{}^p = f_c\,K_c{}^p + f_s\,K_s{}^p \quad (2)$$

where:

$\epsilon$ ....................... porosity
$K$ ...................... saturated hydraulic conductivity
$f_c$ ...................... volume fraction concrete
$f_s$ ...................... volume fraction soil = $(1 - f_c)$
$p$ ....................... factor used to choose either:
arithmetic ($p = 1$),
geometric ($p \rightarrow 0$), or
harmonic ($p = -1$) blending
$b$ ....................... blend
$c$ ....................... concrete
$s$ ....................... soil

Saturation and hydraulic conductivity for a composite material as functions of suction pressure ($\psi$) are calculated from the equations:

$$[\epsilon_b\,S(\psi)_b]^p = f_c\,[\epsilon_c\,S(\psi)_c]^p + f_s\,[\epsilon_s\,S(\psi)_s]^p \quad (3)$$

$$[K_b\,k_h(\psi)_b]^p = f_c\,[K_c\,k_h(\psi)_c]^p + f_s\,[K_s\,k_h(\psi)_s]^p \quad (4)$$

where:

$k_h(\psi)$ ............ hydraulic conductivity as a function of suction pressure
$S(\psi)$ ............ saturation as a function of suction pressure
$\psi$ .............. suction pressure

Example results for hydraulic conductivity obtained by blending E-Area Vault Concrete and OSC1 using arithmetic averaging are shown in Figure 5-5. Using this blending method, a small amount of soil significantly alters the hydraulic conductivity. This occurs because the method is making a homogeneous blend and a small amount of soil leads to a large increase in water flow through a homogeneously mixed material. With arithmetic blending the material with the largest conductivity is weighted the highest. Using the harmonic blending method gives the results shown in Figure 5-6. In this case, concrete properties are more heavily weighted. With harmonic blending, the material with the smallest conductivity is weighted the highest. Years in both figure legends correspond with the concrete-soil blends in Table 5-2.

Since neither of the blending methods demonstrated in Figure 5-5 and Figure 5-6 appeared to represent concrete degradation satisfactorily, the geometric averaging was employed using Eqns. (3) and (4) with a small value of the factor $p$ ($p = 0.01$). Results obtained using this blending method are shown in Figure 5-7 and Figure 5-8. These results appeared to show a reasonable blending to represent the change in concrete properties over time and were adopted for use in the LAWV model. Figure 5-9 and Figure 5-10 show the hydraulic conductivity and water saturation curves obtained by blending a mixture of 90% E-Area Vault Concrete and 10% Gravel with OSC1, respectively. The mixture of 90% concrete with 10% gravel was used to model cracked concrete. Blending this mixture with soil was then used to model degradation of the cracked concrete.

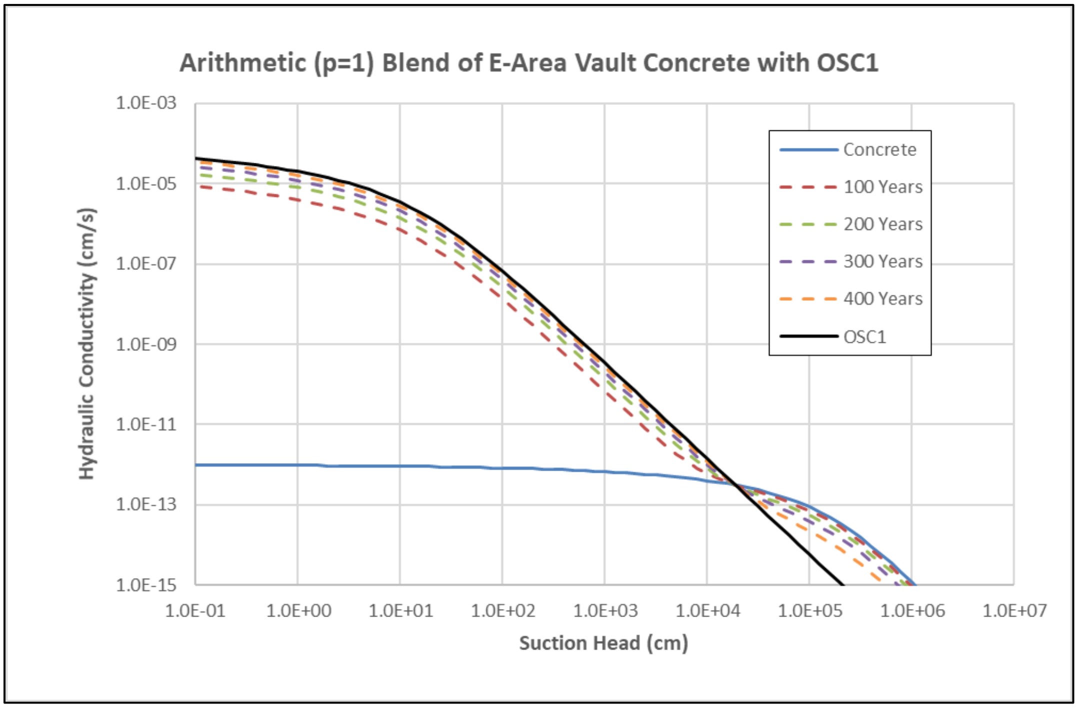


**Figure 5-5 Hydraulic conductivity for blends of E-Area vault concrete with OSC1 calculated using arithmetic averaging.**

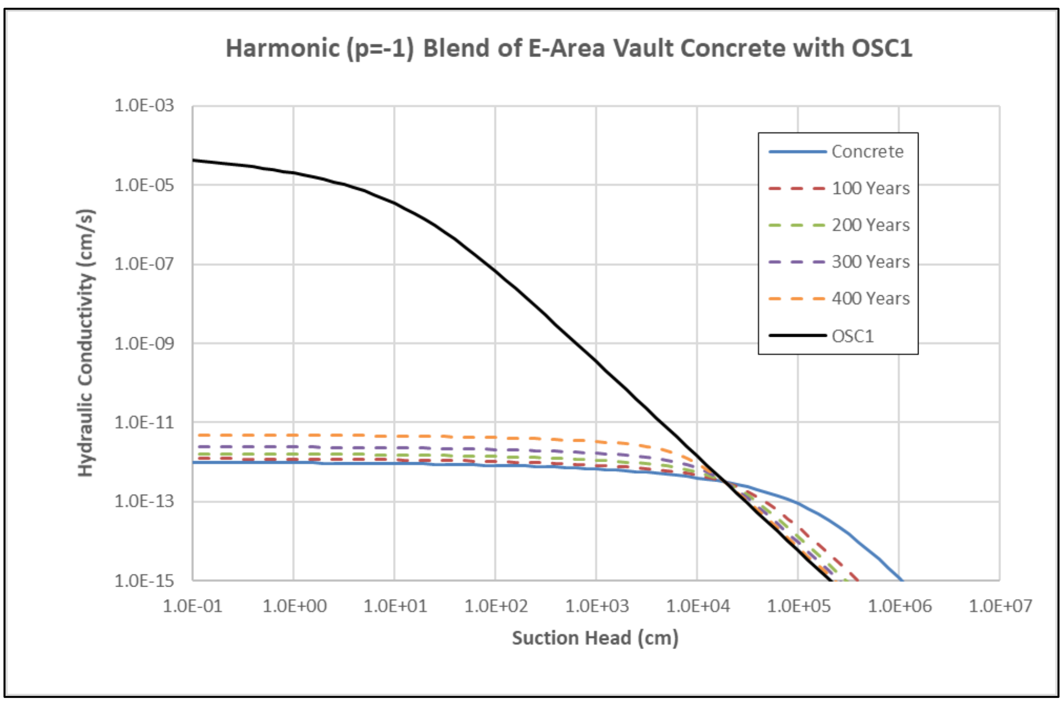


**Figure 5-6 Hydraulic conductivity for blends of E-Area vault concrete with OSC1 calculated using harmonic averaging.**

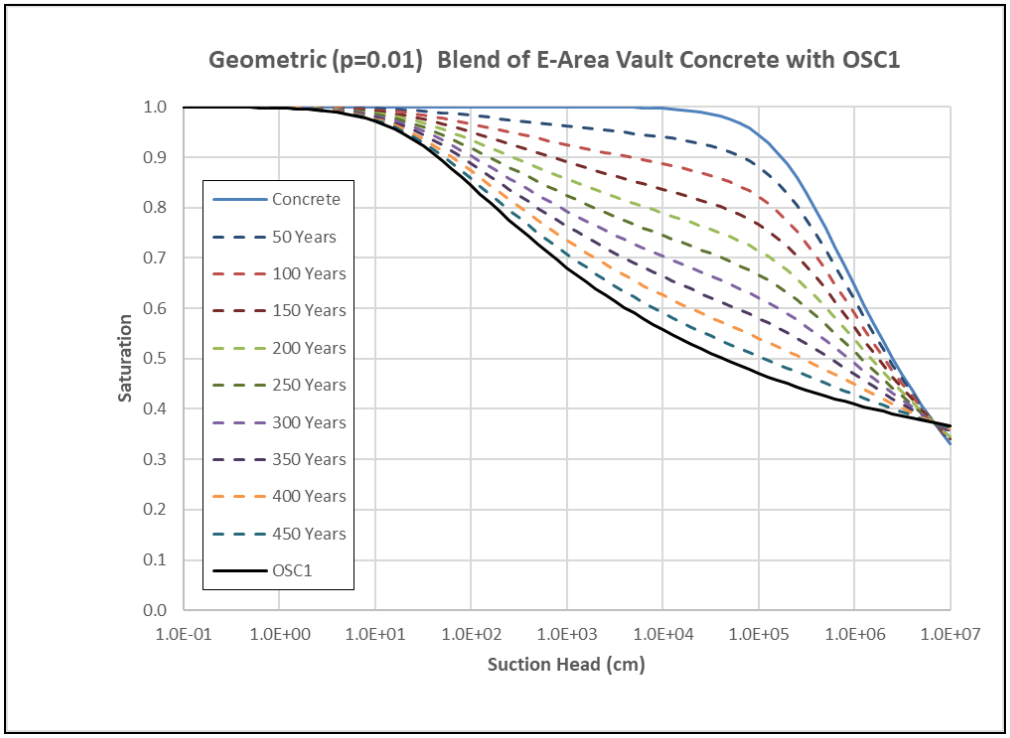


**Figure 5-7 Hydraulic conductivity for blends of E-Area vault concrete with OSC1 calculated using geometric averaging.**

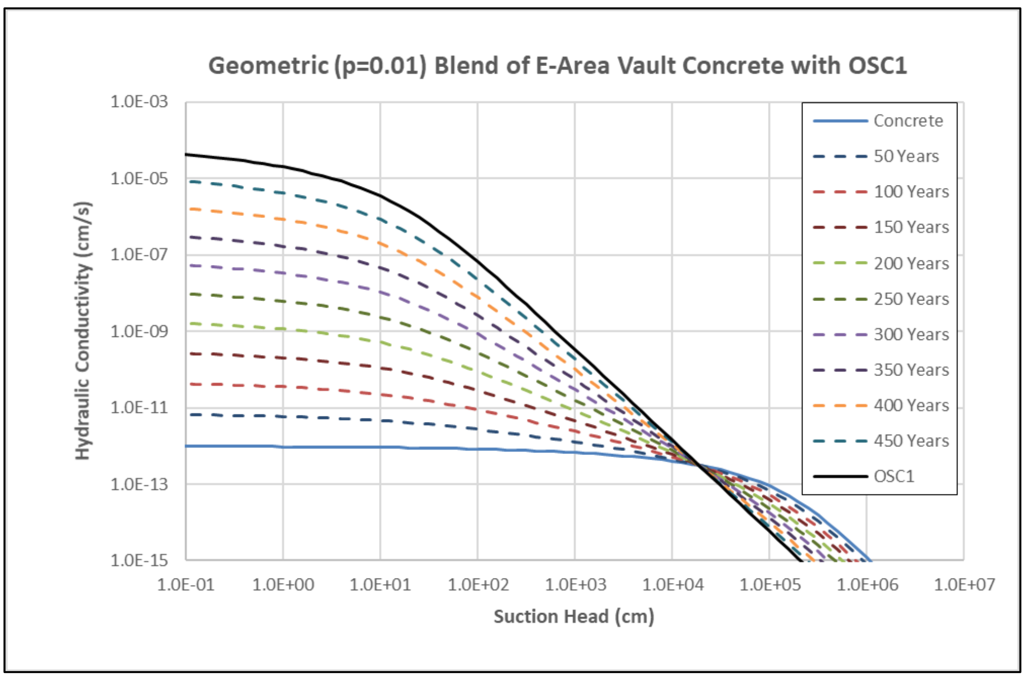


**Figure 5-8 Water saturation for blends of E-Area vault concrete with OSC1 calculated using geometric averaging.**

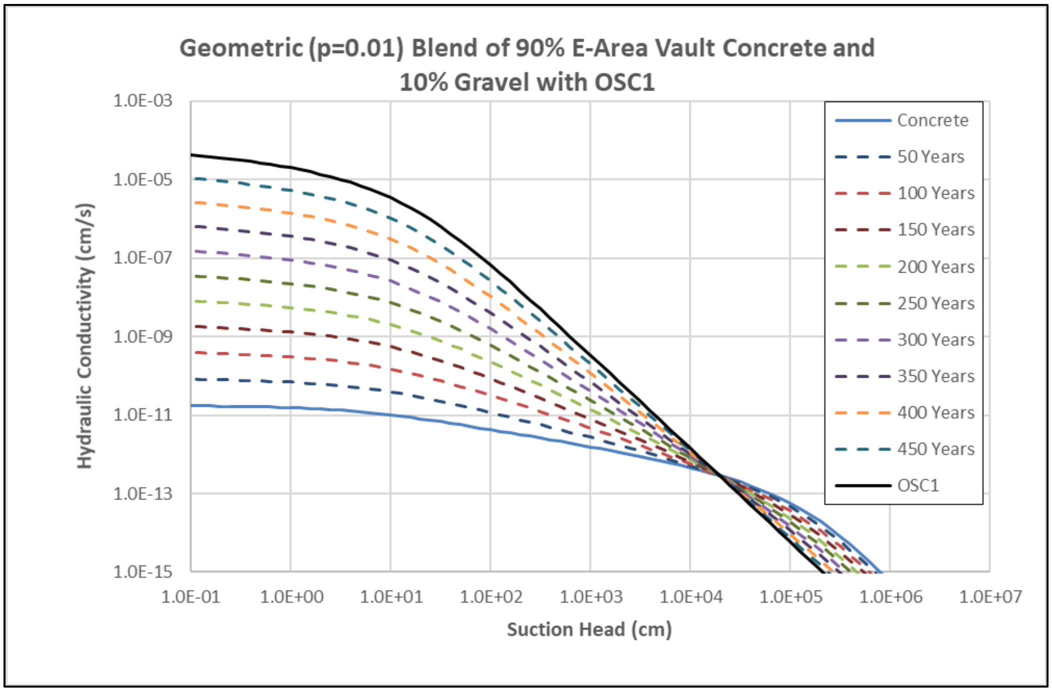


**Figure 5-9 Hydraulic conductivity for blends of 90% E-Area vault concrete and 10% Gravel with OSC1 calculated using geometric averaging.**

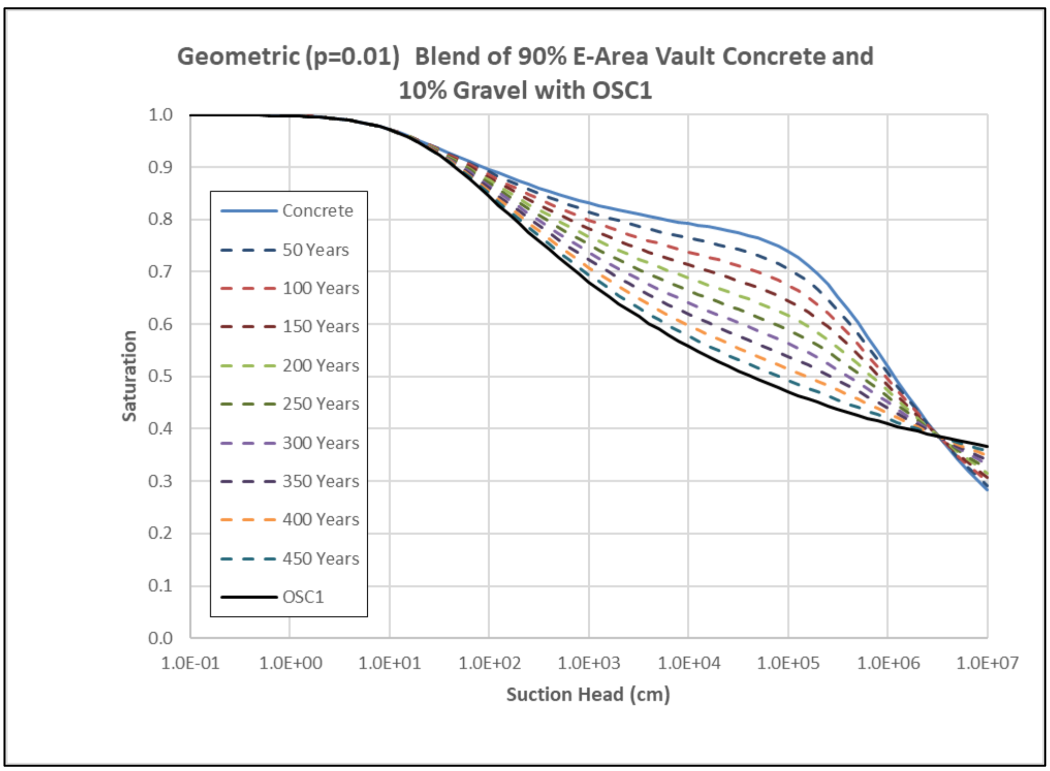


**Figure 5-10 Water saturation for blends of 90% E-Area vault concrete and 10% Gravel with OSC1 calculated using geometric averaging.**

# 6.0 Preliminary LAWV Modeling Results

## 6.1 Vadose Zone Flow

PORFLOW modeling is used to calculate a steady-state flow field for each of the 34 time intervals listed in Table 5-1. Starting times for each interval are listed in the fourth column of Table 5-1. Therefore, for example, the first flow time is from 0 to 171 years, the second time is from 171 to 221 years and so on down the table. "Years" as shown in the figure captions and used in this section are time from the start of LAWV operations in 1994.

Results obtained from the modeling include suction pressure, water saturation of the materials, and flow field throughout the computational domain. In addition, information on the deviation of saturation from the water retention curves and convergence of the flow calculations can be obtained to verify model accuracy. Results for the steady-state flow fields are presented in this section of the report and plots of water saturation and pressure are consigned to Appendices A and B, respectively. Plots of the steady-state flow field based on Darcy velocity for 20 simulation time periods are shown in Figure 6-1 through Figure 6-10. The plots include the first 14 time intervals, time intervals 18, 22, 26 and 30 and the final two intervals. To reduce the number of figures and figure captions, each figure has flow plots for two time intervals. The corresponding infiltration flows calculated by HELP modeling are listed in Table 5-1. The progressive deterioration in the hydraulic behavior of both the closure cap and vault concrete over the simulation time are evident in these figures. The 500-year period from 171 years to 671 years is the time during which degradation of the vault concrete is modeled as described in Section 5.3. The 1000-year period of performance is from 171 years to 1171 years.

Figure 6-1 shows flow fields from the start of LAWV operations (Time 0) until the end of institutional control and for the first 50 years following installation of the final closure cap. The final closure cap is placed over the vault in year 171 beginning the 1000-year compliance period. For the first 50 years the vault concrete is modeled as intact E-Area Vault Concrete. As described in Section 5.1, the PORFLOW two-dimensional model domain extends 20 feet on both sides of the vault. For the first 171 years, the model is run with the soil cover in place which is not physically correct. The infiltration is set to the low value of 0.001 inch/year over the vault and the nominal General Separations Areas (GSA) background infiltration rate of 15.78 inches/year over the 20-ft side areas. This is intended to model the presence of the rain cover on the roof and the gutter/downspouts that collect runoff from the roof and send it to the sump. The drainage system prevents runoff from the roof adding to infiltration water on the sides of the vault. The first plot in Figure 6-1 shows background flow beside the vault and only a very small flow through the vault (markers in the streamlines are spaced every 1000 years) for the first 171 years. Water creep into the vault is more prevalent on the north side where the roof slope is shallower. The plot shows that while the model for this time period is not entirely accurate it still gives reasonable results. Following closure cap placement at 171 years, the second plot in Figure 6-1 shows very small flow throughout the entire computational domain.

Predicted flow fields for the first 100 years when degraded performance of the vault concrete and closure cap are modeled are shown in Figure 6-2. During this time, the closure cap is still performing well, the concrete is relatively intact (10% and 20% soil), and infiltration through the vault is small. Time markers in Figure 6-2 are placed at 300-year and 200-year intervals. Therefore, while the figures show channeling of water to the sides and below the vault, the actual flow through the vault is still very small. The second plot in Figure 6-2 begins to show water flow through the side walls. Figure 6-1 and Figure 6-2 show that flow on the south side of the vault is being drawn underneath the vault because the concrete is blocking water flow directly into this region creating suction beneath the vault.

Figure 6-3 shows water flow fields from 321 years to 421 years. During this time, the concrete (30% and 40% soil) and closure cap continue to degrade. There is more water flow through the vault and the water is moving faster with 100-year and 80-year time markers. The second plot in Figure 6-3 (200 to 250 years after the closure cap is placed) shows that the stream traces are beginning to straighten out indicating more uniform water flow through the entire region. The increase in flow and trend to more uniform flow continues in Figure 6-4 which shows the flow fields from 421 years to 521 years. In these two plots, the concrete is now mixed with 50% and 60% soil. Flow through the closure cap is still only approximately 0.5 to 1.5 in/year so the trend to more uniform flow is primarily from concrete degradation.

By 671 years, hydraulic properties of the LAWV concrete in the roof, floor and walls have degraded to those of uncompacted operational soil cover. The vault concrete is fully degraded by the last plot in Figure 6-6. Thereafter, flow increases as closure cap performance degrades (see infiltration listed in Table 5-1). Figure 6-5 through the first plot in Figure 6-10 show a steady increase in flow through the vault as the closure cap fails. The vault roof is assumed to collapse at 2976 years increasing flow through the vault region as runoff from the intact closure cap enters the space created by the roof collapse. This effect can be seen in Figure 6-10 where the first plot is prior to roof collapse and the second plot is after. The longer distance between flow markers within the vault in the second plot indicates the increased flow. Beyond 2976 years, the flow pattern is assumed to remain unchanged.

Plots of suction pressure and water saturation in the LAWV vadose zone at the same time intervals are shown in Appendices A and B, respectively.

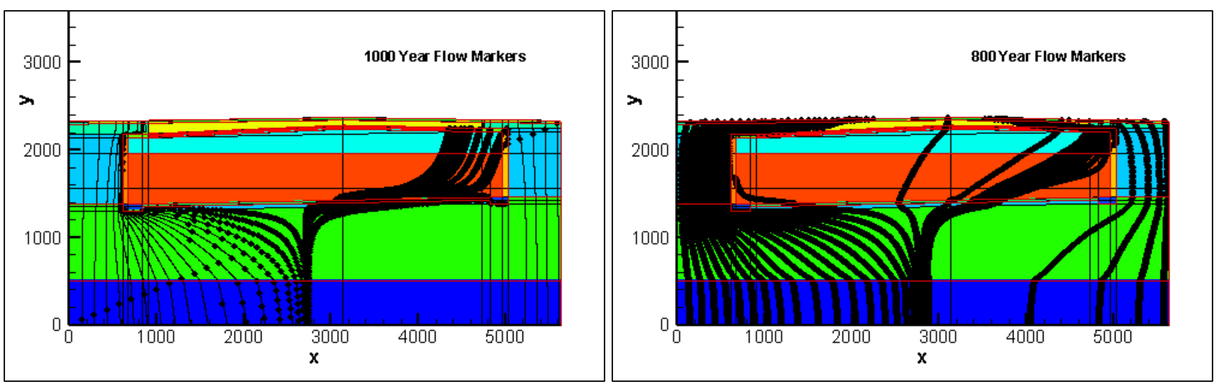


**Figure 6-1 LAWV Flow Fields for 0 – 171 and 171 – 221 years.**

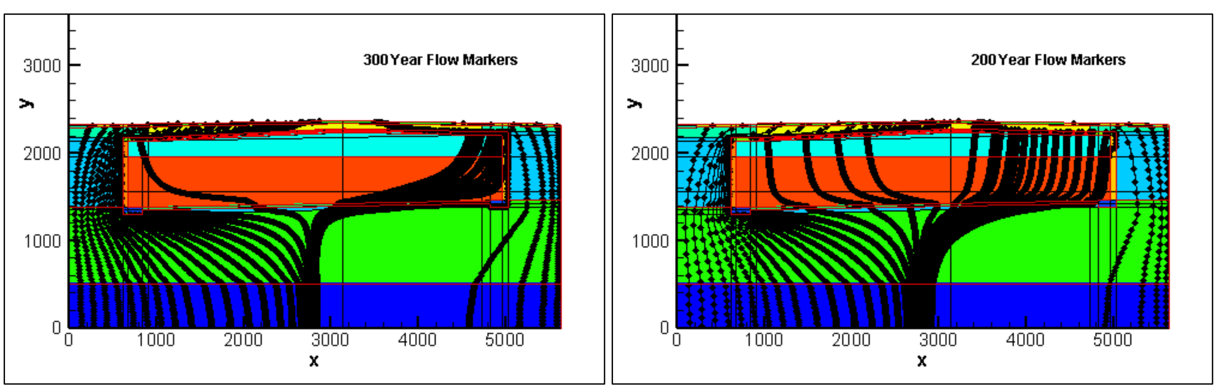


**Figure 6-2 LAWV Flow Fields for 221 – 271 and 271 – 321 years.**

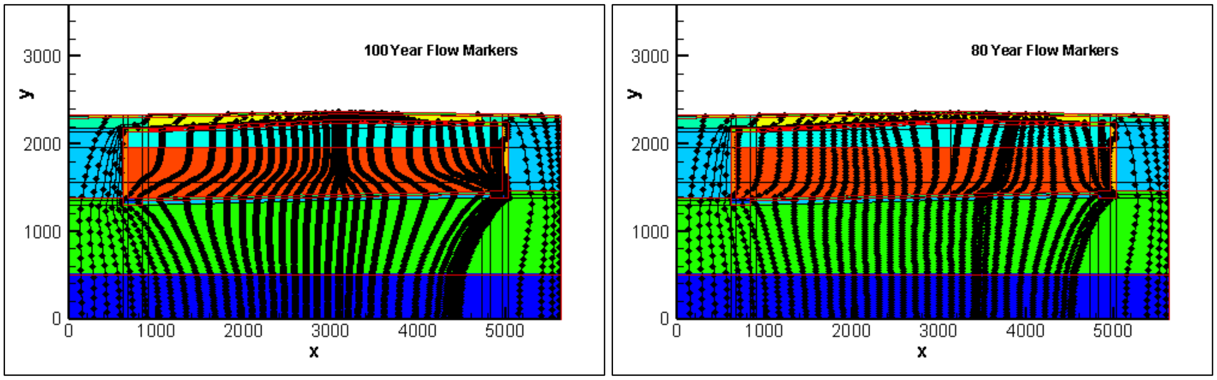


**Figure 6-3 LAWV Flow Fields for 321– 371 years and 371 – 421 years.**

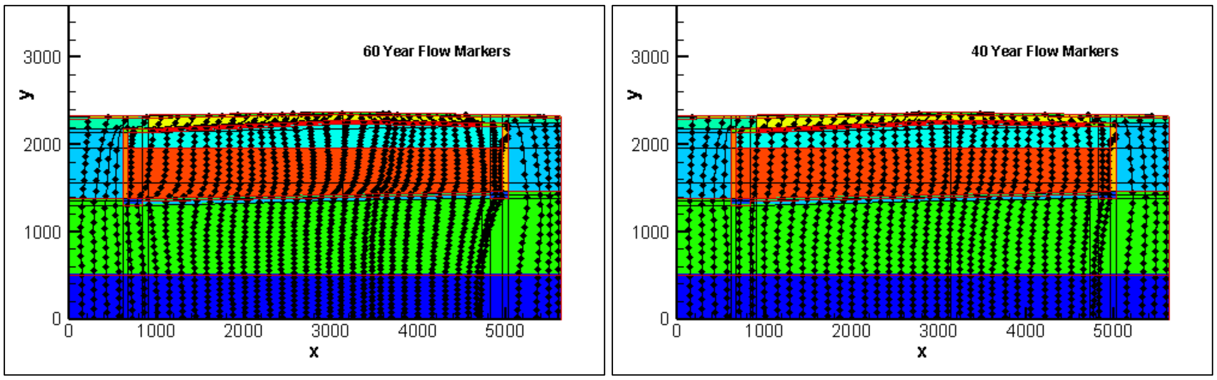


**Figure 6-4 LAWV Flow Fields for 421 – 471 years and 471 – 521 years.**

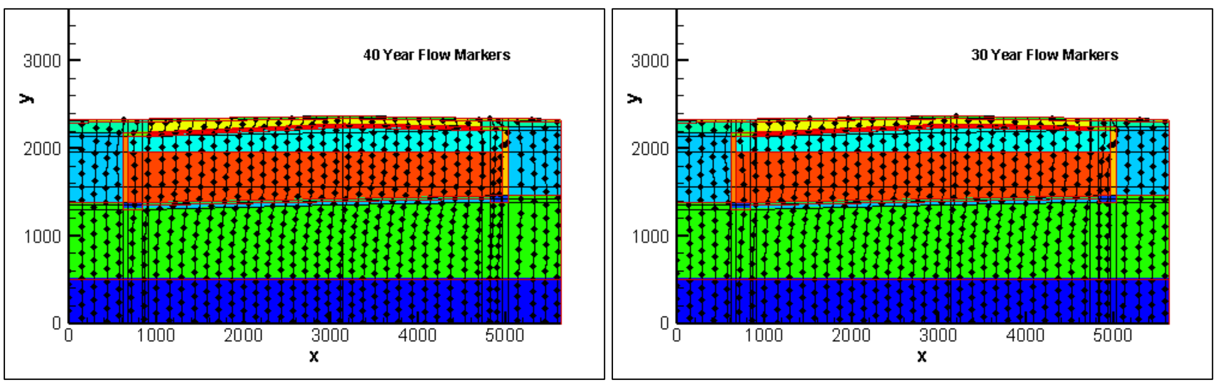


**Figure 6-5 LAWV Flow Fields for 521 – 571 years and 571 – 621 years.**

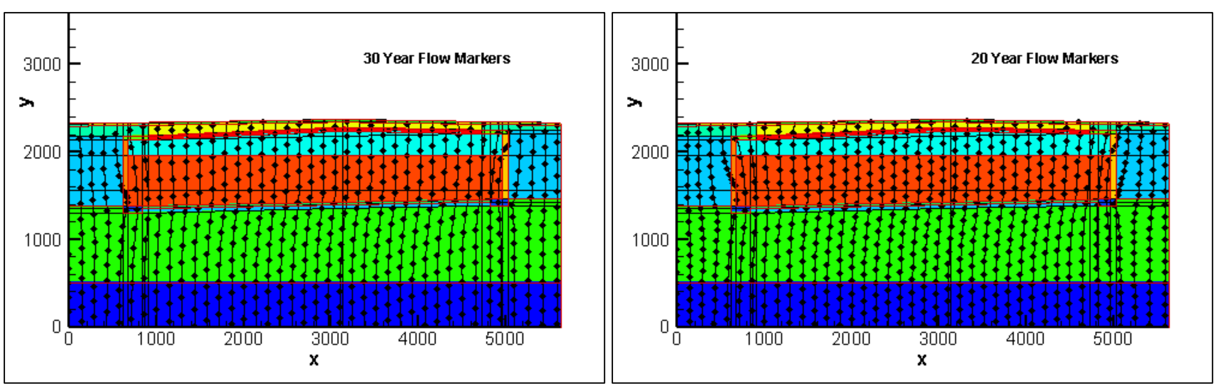


**Figure 6-6 LAWV Flow Fields for 611 – 671 years and 671 – 721 years.**

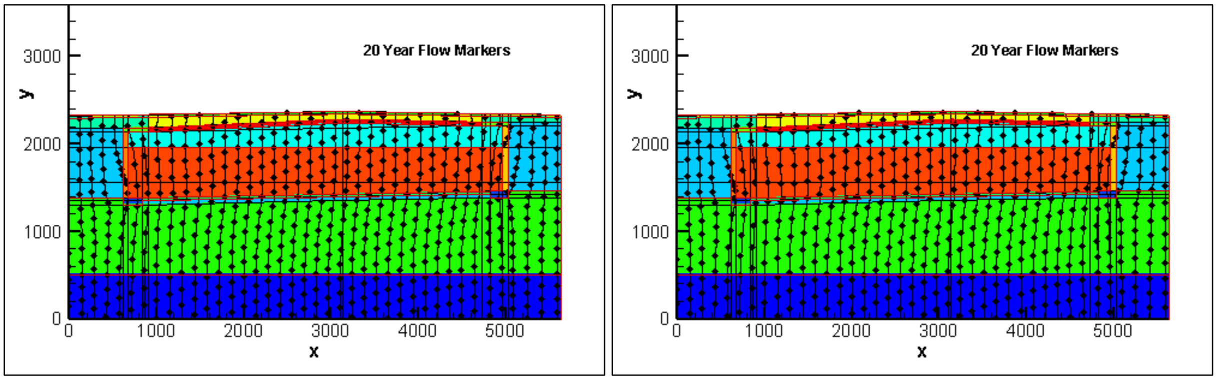


**Figure 6-7 LAWV Flow Fields for 721 – 771 years and 771 – 821 years.**

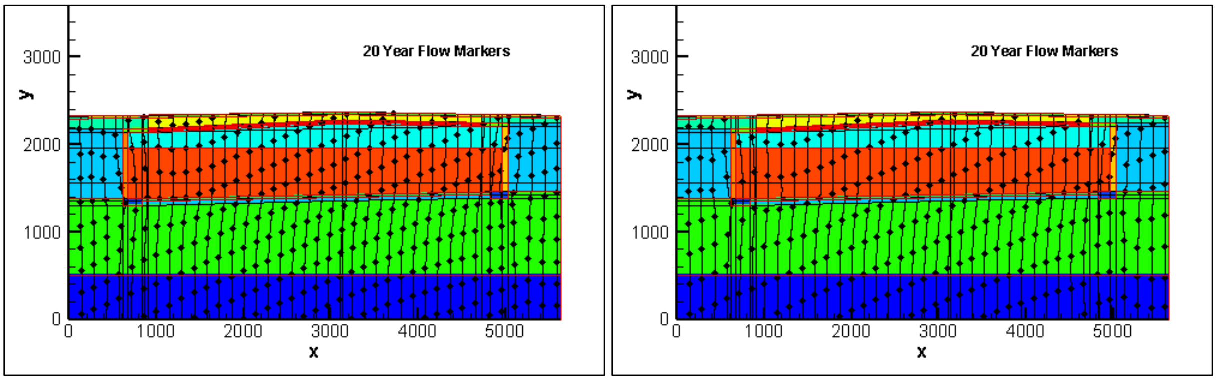


**Figure 6-8 LAWV Flow Fields for 971 – 1021 years and 1171 – 1321 years.**

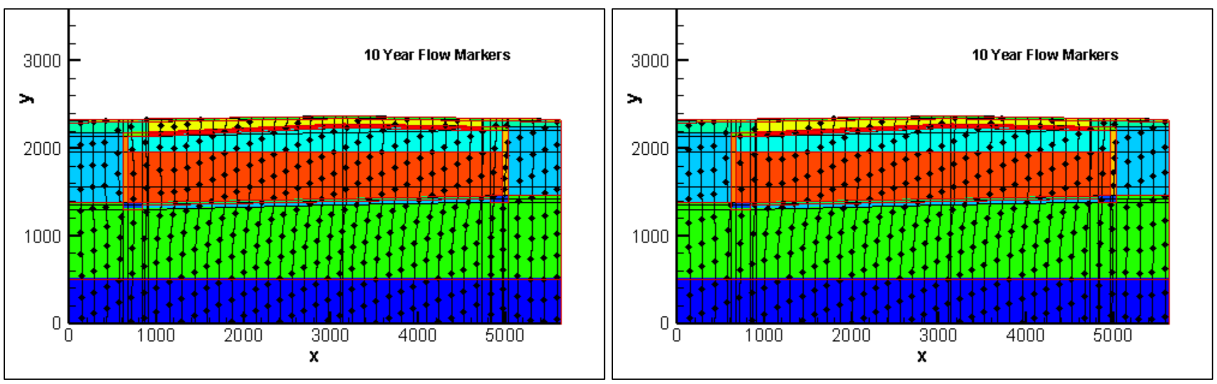


**Figure 6-9 LAWV Flow Fields for 1771 – 1921 years and 2371– 2521 years.**

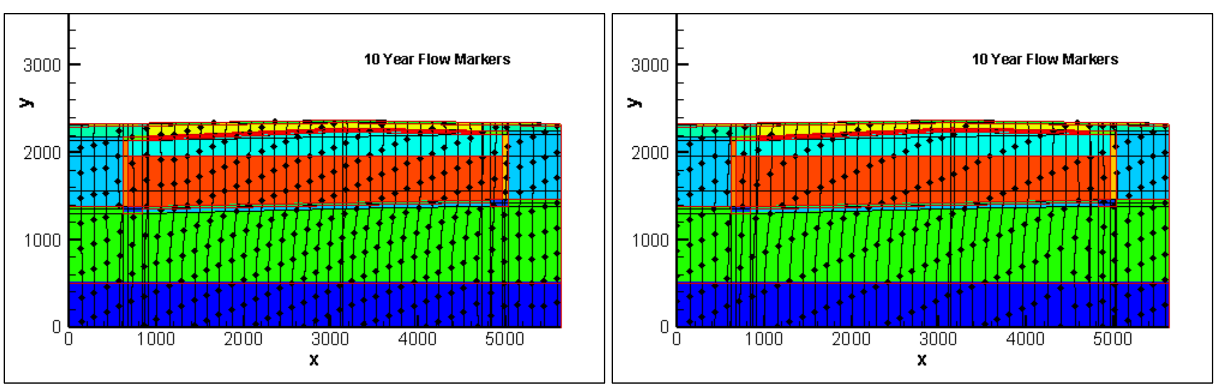


**Figure 6-10 LAWV Flow Fields for 2821 – 2976 years and >2976 years.**

## 6.2 Radionuclide Transport

LAWV transport calculations were made for the following nine parent radionuclides and daughters:

C-14, Cl-36, H-3, I-129, Nb-94, Np-237 (U-233, Th-229),
Tc-99, U-235 (Pa-231, Ac-227) and Zr-93 (Nb-93m).

These radionuclides were chosen as those giving a significant dose from LAWV disposal and therefore having relatively small disposal limits in the 2008 PA. I-129 is a useful radionuclide to include for testing transport calculations because it has both a long half-life and small $K_d$. This combination of properties ensures that the I-129 peak will be quickly observed and that the area under the peak should equal the amount of I-129 initially deposited.

One mole (mol) of each parent radionuclide was distributed uniformly in the waste zone and the resulting flux to the water table (mol/yr) calculated over a 50,000-year time period. The parent radionuclides were introduced at the start of LAWV operations. At 2976 years following the start of LAWV operations, when structural analysis predicts the vault roof will collapse, the existing waste inventory is relocated to the lower 4.5 feet of the waste zone. This is intended to mimic the consolidation of waste containers within the collapsed vault.

### *6.2.1 $K_d$ Properties*

Solid-liquid distribution coefficients ($K_d$) were obtained from the latest Geochemical Data Package (Kaplan, 2016). As specified in the data package (Section 5.2 Table 7), reducing cement $K_d$ values were used for LAWV concrete. The model used clayey sediment $K_d$ values in the waste zone and upper vadose zone and sandy sediment $K_d$ values in the lower vadose zone. The data package recommends using $K_d$ values impacted by cementitious leachate in the waste zone and upper and lower vadose zone soils. However; an annotation to the table states that the use of cementitious leachate impacted $K_d$ in the waste and vadose zone regions below the vault has not been formally evaluated for use in the PA baseline. The 2008 PA model did not use cementitious leachate impacted $K_d$ values in vadose zone soil or the waste region. Therefore, these preliminary calculations also do not use soil and waste $K_d$ values with cementitious leachate factors applied.

### *6.2.2 Concrete Aging*

Concrete $K_d$ values vary as concrete ages (Kaplan, 2016). Concrete aging is related to the number of pore volume exchanges made as water flows through the material. The 2016 chemical data package recommends using the following concrete aging:

- Stage I (young) concrete lasts for 50 exchange cycles
- Stage II (middle) concrete lasts for 500 exchange cycles
- Stage III (aged) concrete lasts 4000 exchange cycles

After 4000 pore volume exchanges, concrete $K_d$ values are assumed to become those for clayey soil. For this model assessment, a relatively simple method was used to estimate pore volume exchanges. For the LAWV roof and floor and the waste zone, average vertical velocities from the PORFLOW calculations during each flow period shown in Table 5-1 were used to determine the number of pore volume exchanges. For the LAWV walls the average horizontal velocity was used. The cumulative number of pore volume exchanges was tracked through each flow step and the times calculated when the exchange volumes reached the end of each stage. Table 6-1 gives the resulting times when concrete stage changes occur. The concrete was aged to the next level at the start of the time step where the number of exchange cycles was reached.

**Table 6-1 LAWV Concrete Aging Times in Years from Start of Operations**

| | Roof and Roof Beams | Floor and Wall Footers | North Wall | South Wall | Waste |
|---|---|---|---|---|---|
| Stage I to II | 771 | 771 | 1171 | 1171 | 2071 |
| Stage II to III | 1121 | 1121 | >2976 | >2976 | >2976 |
| Stage III - Soil | >2976 | >2976 | >2976 | >2976 | >2976 |

The results in Table 6-1 are in reasonably good agreement with concrete aging times used in the 2008 PA. The 2008 PA differentiated between cracked and uncracked concrete. For cracked concrete, which would be most like the current model, all LAWV concrete was aged from Stage I to Stage II at 640 years, from Stage II to Stage III at 1264.5 years, and the concrete $K_d$ transitioned to soil at 4689.5 years. A conceptual difference between the two models is that the 2008 PA assumed concrete $K_d$ values remain active until 4000 pore volume exchanges have been made while the current model changes concrete $K_d$ values to those of soil when the vault roof collapses.

### *6.2.3 Radionuclide Flux to Water Table*

Graphs of flux to the water table (mol/yr) for the nine parent radionuclides and daughters with half-lives greater than one year used for the LAWV vadose zone model evaluation are shown in Figure 6-11 through Figure 6-16. Figure 6-14 through Figure 6-16 show the parent and daughter radionuclides on both linear and semi-log scale plots to include progeny at low levels. Table 6-2 compares the maximum flux and the time when the maximum flux occurs for all radionuclides. Times in these figures and the table are measured from the time LAWV operations start in 1994. The sharp peaks in flux for C-14, Tc-99, Np-237, Pa-231 and Ac-227 all occur at about 3000 years, soon after LAWV roof collapse when a significant increase in infiltration flow through the vault area takes place. Concentration profiles showing C-14 transport through the LAWV vadose zone at simulation times between 50 and 12,000 years are presented in Appendix C along with a brief discussion of those results. The results are discussed further when they are compared to the 2008 PA results in Section 6.2.4.

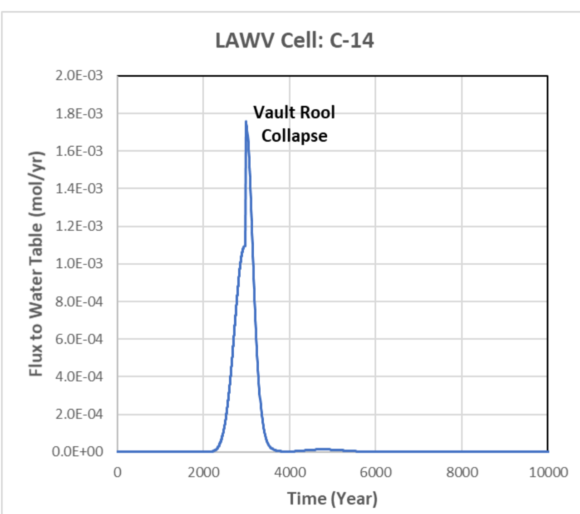


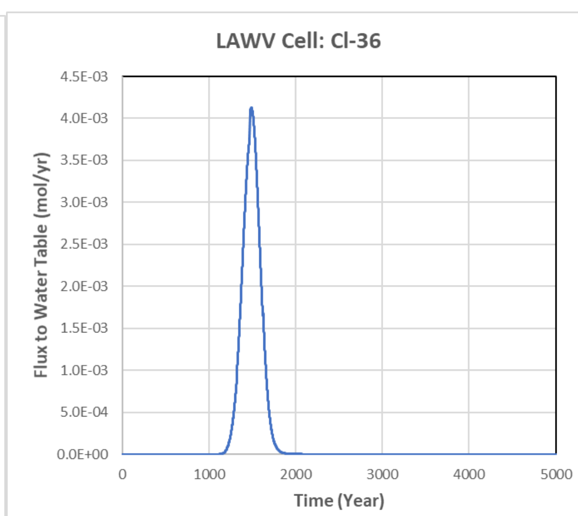


**Figure 6-11 Linear plot of flux to water table for C-14 and Cl-36.**

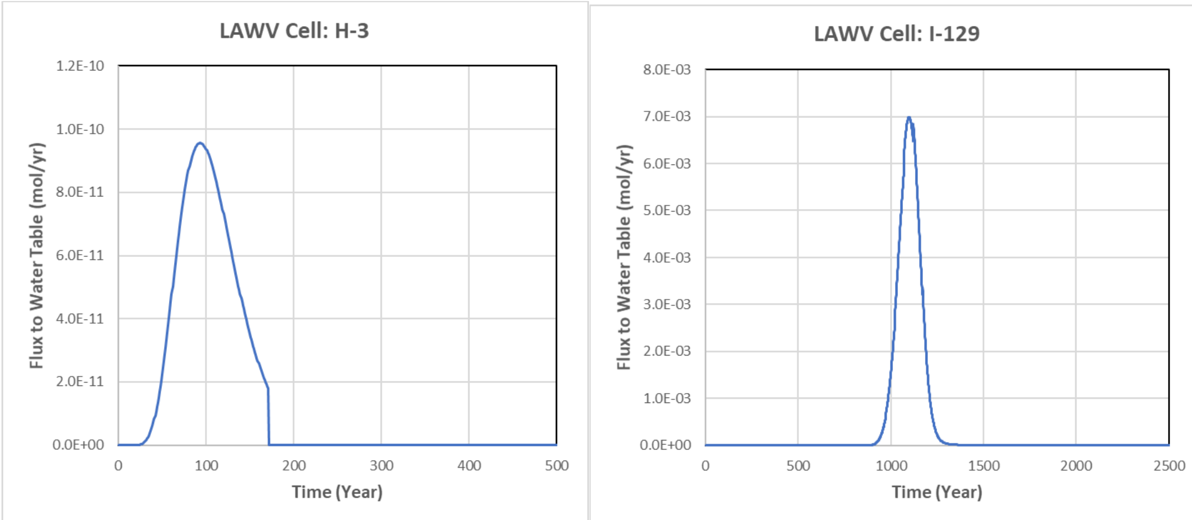


**Figure 6-12 Linear plot of flux to water table for H-3 and I-129.**

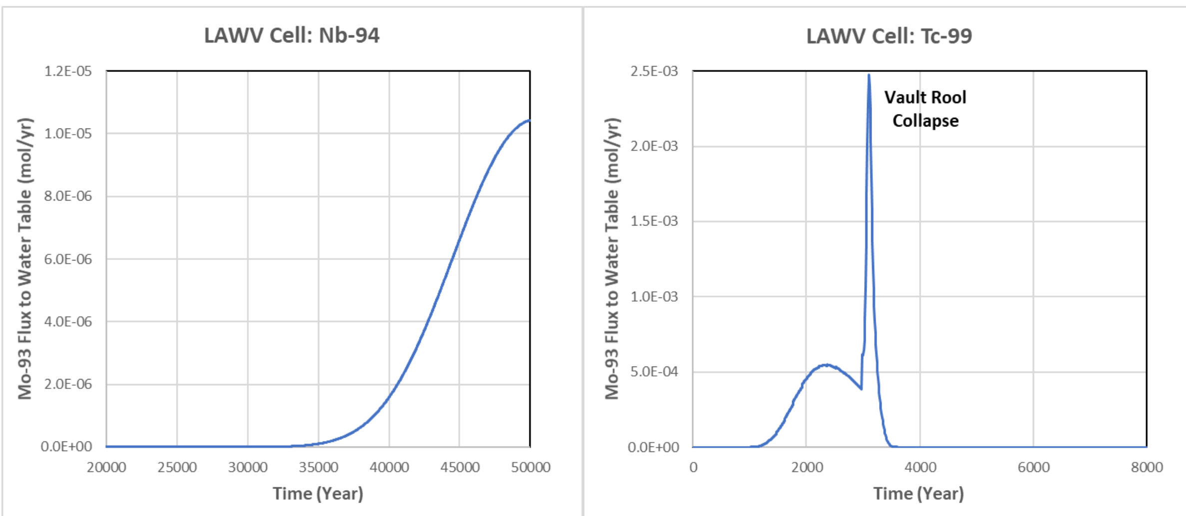


**Figure 6-13 Linear plot of flux to water table for Nb-94 and Tc-99.**

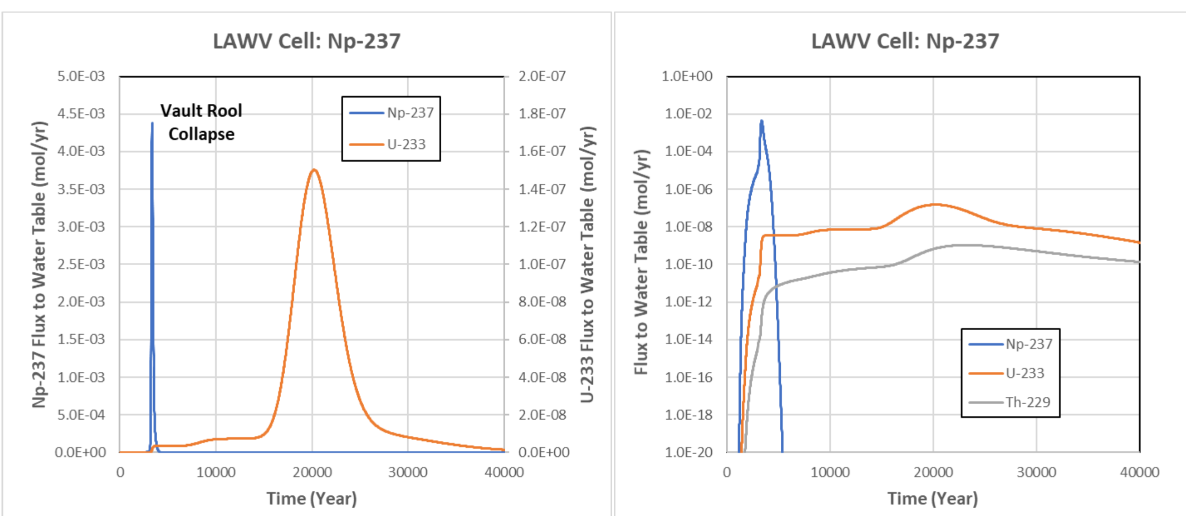


**Figure 6-14 Linear and semi-log plots of flux to water table for Np-237 and daughters.**

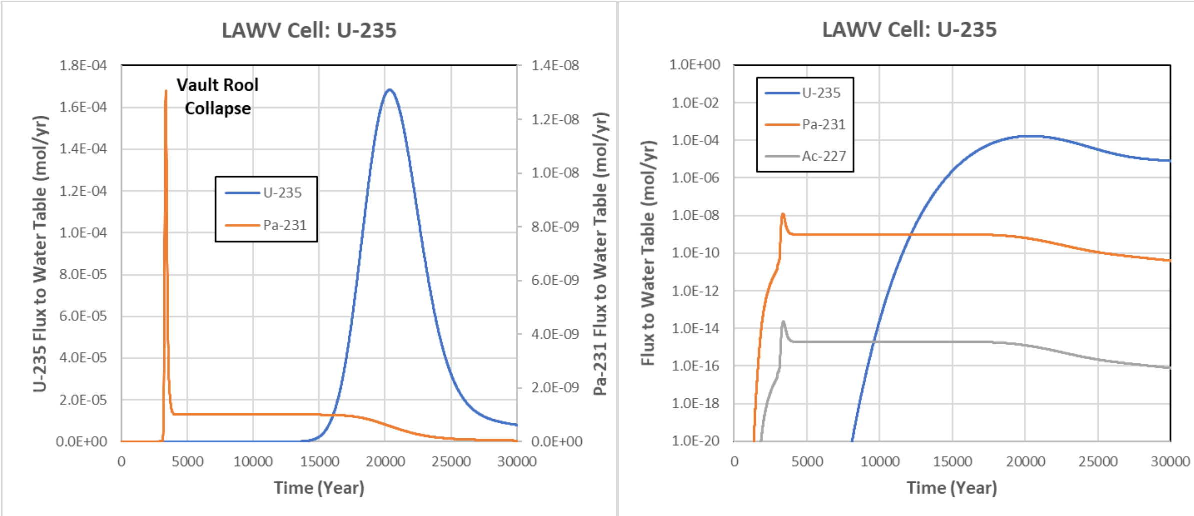


Figure 6-15 Linear and semi-log plots of flux to water table for U-235 and daughters.

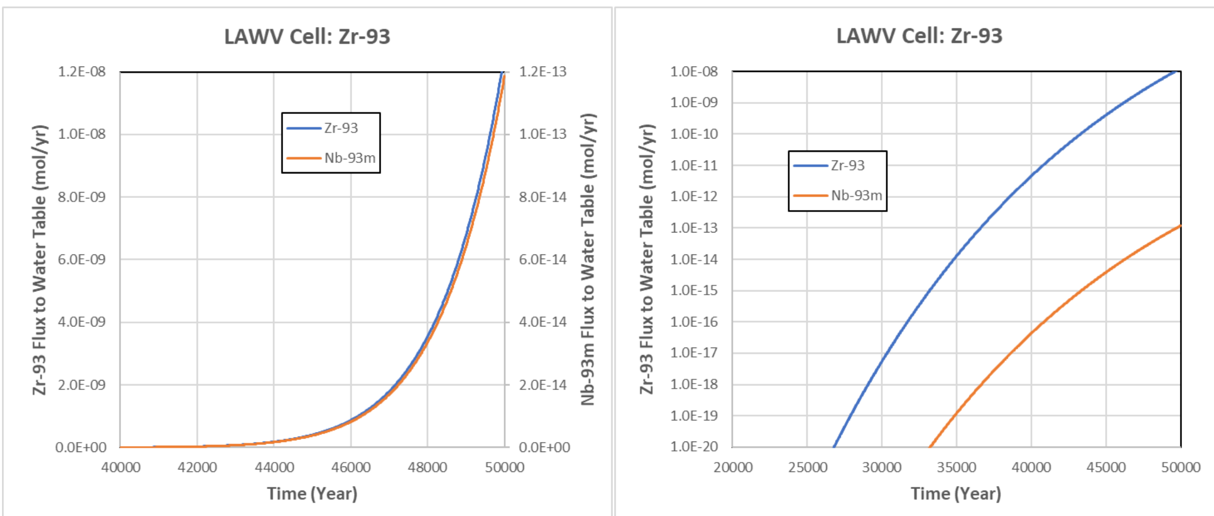


Figure 6-16 Linear and semi-log plots of flux to water table for Zr-93 and Nb-93m.

**Table 6-2 Maximum Flux to Water Table and Time of Maximum Flux**

| Nuclide | Max mol/yr | Year | Nuclide | Max mol/yr | Year |
|---|---|---|---|---|---|
| **C-14** | 1.76E-03 | 2986 | **Np-237** | 4.38E-03 | 3366 |
| **Cl-36** | 4.13E-03 | 1488 | *U-233* | 7.14E-11 | 20236 |
| **H-3** | 9.56E-11 | 93 | *Th-229* | 1.06E-09 | 23136 |
| **I-129** | 6.99E-03 | 1099 | **U-235** | 1.68E-04 | 20356 |
| **Nb-94** | 1.04E-05 | 50000 | *Pa-231* | 1.31E-08 | 3366 |
| **Tc** | 2.48E-03 | 3106 | *Ac-227* | 2.36E-14 | 3396 |
| | | | **Zr-93** | 1.25E-08 | 50000 |
| | | | *Nb-93m* | 1.19E-13 | 50000 |

*6.2.4 Comparison to 2008 PA*

*Timeline*. In the current LAWV model, time zero is the start of operations in 1994 and the end of ELLWF operations is expected to be in 2065. This is an operational span of 71 years after which the 100-year period of institutional control begins. The 2008 PA calculations assumed ELLWF operations would end and institutional control begin in 2020, which was used as time zero in the flow modeling. The 2008 model placed waste in the LAWV 12.5 years prior to closure which was taken to be the midpoint of operations assuming LAWV operations began in 1995. It appears that the 2008 PA transport calculations shift time zero to be when the waste was placed. That would place time zero for the 2008 PA transport modeling in calendar year 2007.5 versus 1994.74 in the current model. To be on the same calendar year scale 12.5 years was added to the relative 2008 PA transport times. This small correction makes little difference except for tritium where it is almost exactly one half-life. The difference of 45 years in LAWV operation between the two models (i.e. the closure cap is placed 45 years earlier in the 2008 PA calculation) makes a direct comparison of results difficult.

*Vadose Zone.* 40.5 ft depth in 2008 PA model versus 46.8 ft depth in current model.

*Infiltration*. Figure 6-17 compares the LAWV infiltration over the vault used in the 2008 PA with the interpolation of the 2019 calculation (Dyer, 2019) used for the present modeling. Both calculations were made with the same version of the HELP model. The 2019 infiltration falls below the 2008 values during the first 600 years. Lower infiltration would slow the transport of radionuclides through the LAWV vadose zone. The most significant change between the 2008 PA model and 2019 closure cap design is that an HDPE geomembrane liner has been added above the geosynthetic clay layer in the most recent version. The geomembrane provides the primary barrier to water infiltration in the current HELP modeling. LAWV roof collapse at 2976 years results in a large increase in flow through the vault area as runoff from the intact closure cap enters the cavity created by vault failure and waste subsidence. The 2008 PA chose to model roof collapse at 1900 years to more easily capture peak radionuclide concentrations in out years.

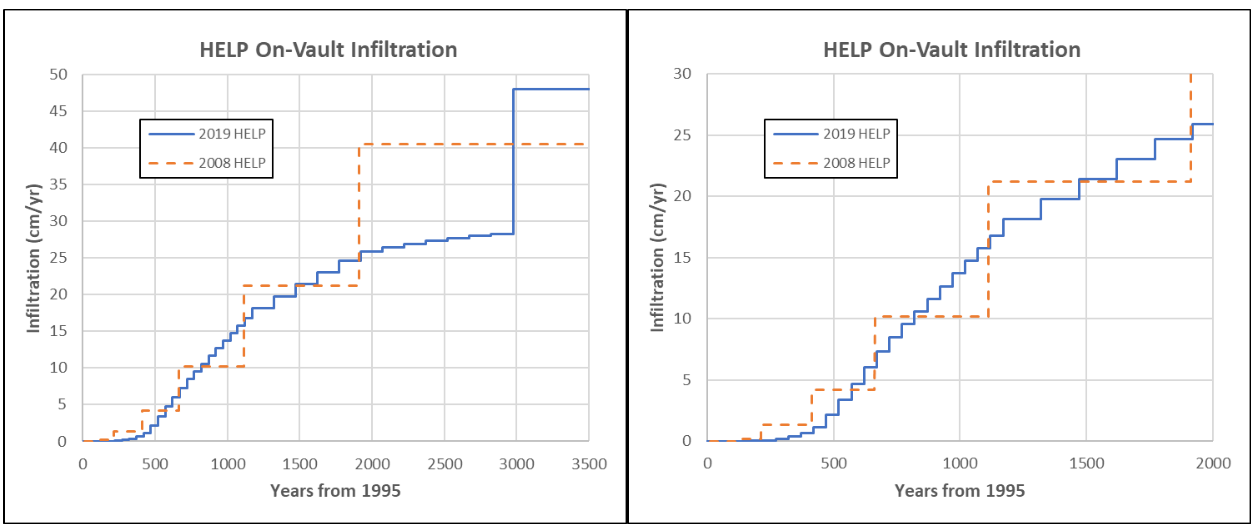


**Figure 6-17 HELP LAWV infiltration for 2008 PA and 2019 revision.**

*Concrete Degradation*. The method used to model concrete degradation and cracking in the current LAWV model is described in Sections 2.1 and 5.3. A different approach was used in the 2008 PA which can be summarized as:

1. The structural analysis was used to determine the extent of concrete cracking.
2. Hydraulic conductivity of the cracks was calculated using standard methods.
3. Like the blending process used in the current model, saturated hydraulic conductivities for cracked concrete were calculated to include enhanced conductivity from the presence of the cracks.
4. Concrete takes soil hydraulic properties when the vault roof collapses.

The LAWV structural analysis predicts static load cracks that do not penetrate the concrete occur over a limited area of the roof slab and walls when the closure cap is placed over the vault. The analysis also predicts separation of the vault walls from the footers within 50 to 100 years after closure and estimates the probability of further concrete cracking from differential settlement. To address the structural findings, LAWV modeling in the 2008 PA used two models. One model was termed the "Uncracked Model" and the other the "Cracked Model". However, both models include concrete cracking that the structural analysis predicted with high certainty while the "Cracked Model" included additional cracking in the vault roof and walls over time. It was assumed that cracking only impacted concrete saturated hydraulic conductivity. Both models were used to predict flux to the water table and composite results were weighted 96.9% "Uncracked" and 3.1% "Cracked". Full details of the models and methods used to calculate saturated hydraulic conductivity are given in Chapter 3 of the 2008 PA (WSRC, 2008).

Table 6-3 lists saturated hydraulic conductivities used for concrete regions in the 2008 PA (WSRC, 2008, Tables 3-9 and 3-10). Cracking was confined to regions of the roof near the walls (80 inches total) and wall regions at the top, bottom, and center of the wall (2 feet each). The current model assumes that all roof, floor and wall concrete is cracked including the roof beams and the wall footers. The 2008 PA also includes a region of high conductivity near the floor to simulate a leak (0.5 inch gap) caused by the separation between the wall and footer. This was not included in the current model. The "Drain" in Table 6-3 is a one foot drainage layer above the roof analogous to the GCL layer in the current model but having a lower hydraulic conductivity. The GCL hydraulic conductivity in the current model ($K_h$ = 1.40E-03 cm/s) was chosen to be close to the conductivity used in the HELP infiltration calculations. Figure 6-18 compares the 2008 PA saturated hydraulic conductivities with values used in the current modeling.

**Table 6-3 2008 PA Concrete Ksat Values.**

| | | Time Period (Years from Start of LAWV Operation) | | | | | | | |
|---|---|---|---|---|---|---|---|---|---|
| | **Cement Region** | 0 - 125 | 125 - 135 | 135 - 225 | 225 - 425 | 425 - 675 | 675 - 1125 | 1125 - 1925 | > 1925 |
| **Uncracked Model** | Cracked Roof | 1.00E-12 | 3.11E-09 | 3.11E-09 | 3.11E-09 | 3.11E-09 | 3.11E-09 | 3.11E-09 | 1.20E-04 |
| | Wall | 1.00E-12 | 3.20E-11 | 3.20E-11 | 3.20E-11 | 3.20E-11 | 3.20E-11 | 3.20E-11 | 1.20E-04 |
| **Cracked Model** | Cracked Roof | 1.00E-12 | 3.11E-09 | 2.43E-06 | 1.03E-05 | 2.24E-05 | 4.12E-05 | 4.37E-04 | 1.20E-04 |
| | Wall | 1.00E-12 | 3.20E-11 | 3.17E-06 | 1.33E-05 | 2.91E-05 | 5.36E-05 | 5.93E-04 | 1.20E-04 |
| **Both Models** | Roof Center | 1.00E-12 | 3.11E-09 | 3.11E-09 | 3.11E-09 | 3.11E-09 | 3.11E-09 | 3.11E-09 | 1.20E-04 |
| | Floor Center | 1.00E-12 | 1.00E-12 | 1.00E-12 | 1.00E-12 | 1.00E-12 | 1.00E-12 | 1.00E-12 | 1.20E-04 |
| | Floor Leak | 1.00E-12 | 1.90E-06 | 1.90E-06 | 1.90E-06 | 1.90E-06 | 1.90E-06 | 1.90E-06 | 1.20E-04 |
| | Drain | 4.09E-05 | 4.09E-05 | 4.09E-05 | 4.09E-05 | 4.09E-05 | 4.09E-05 | 4.09E-05 | 1.20E-04 |

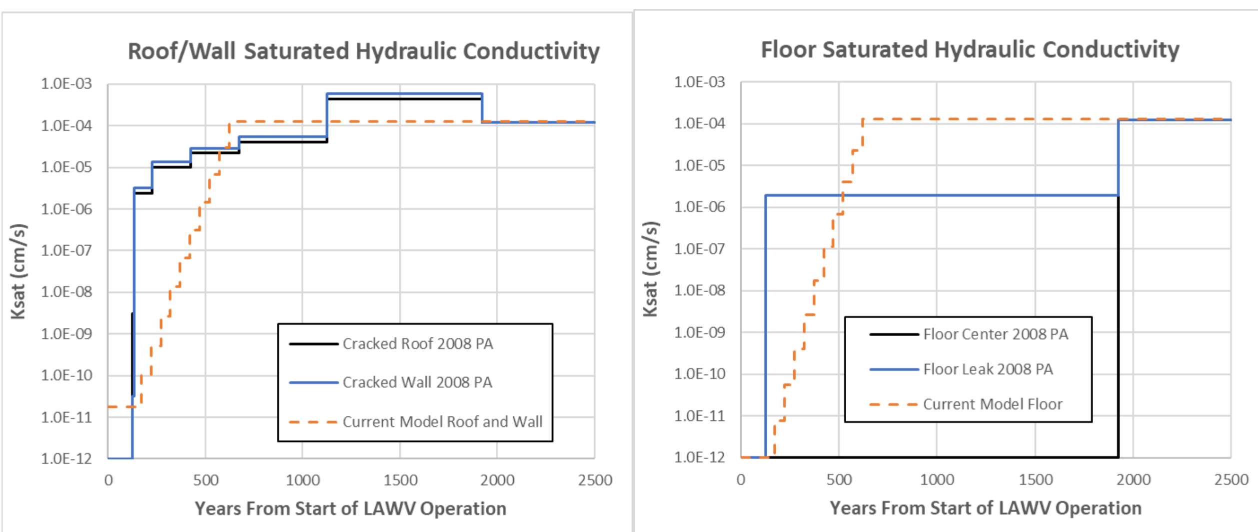


**Figure 6-18 Concrete Saturated Hydraulic Conductivites used in 2008 PA and Current Model.**

*Sorption Properties*. Sorption properties ($K_d$ values) for the radionuclides and significant materials used in this study (Kaplan, 2016) are summarized in Table 6-4 and compared to the values from the 2006 Chemical Database, which was used for the 2008 PA. Tritium is not included in Table 6-4 because it has a $K_d$ of zero for all materials in both databases. $K_d$ values are unchanged for actinium, thorium and zirconium in sandy soil (lower vadose zone) and clayey soil (upper vadose zone, waste and backfill). The trend for other elements is an increase in soil $K_d$ although for protactinium and neptunium the $K_d$ in clayey soil decreases. Iodine, chlorine and technetium are the only elements with a decrease in $K_d$ for Phase I (young) reducing cement. In general, there are significant differences in sorption properties between the two databases which will have a direct effect on radionuclide transport.

In addition to differences in $K_d$ values, the 2008 PA model assumed that the vault concrete retained concrete transport properties after hydraulic failure. $K_d$ values in the concrete regions were changed according to the 50, 500, 4000 pore-volume exchange aging mechanism assuming soil properties only after 4000 pore-volumes passed through each region. In the current model, all the vault concrete takes $K_d$ values of clayey soil following vault roof collapse at 2976 years.

**Table 6-4 Sorption Properties in 2016 and 2006 Chemical Databases.**

| Element | Chemical Database | Sand | Clay | Reducing Cement | | |
|---|---|---|---|---|---|---|
| | | | | Phase I | Phase II | Phase III |
| Ac | 2016 | 1100 | 8500 | 7000 | 7000 | 1000 |
| | 2006 | 1100 | 8500 | 5000 | 5000 | 500 |
| C | 2016 | 1 | 30 | 2000 | 5000 | 50 |
| | 2006 | 0 | 0 | 20 | 10 | 0 |
| Cl | 2016 | 1 | 8 | 0 | 10 | 1 |
| | 2006 | 0 | 0 | 0.8 | 2 | 0 |
| I | 2016 | 1 | 3 | 0 | 2 | 0 |
| | 2006 | 0 | 0.6 | 8 | 20 | 0 |
| Nb | 2016 | 1000 | 1000 | 1000 | 1000 | 500 |
| | 2006 | 0 | 0 | 1000 | 1000 | 500 |
| Np | 2016 | 3 | 9 | 10000 | 10000 | 5000 |
| | 2006 | 0.6 | 35 | 2000 | 2000 | 200 |
| Pa | 2016 | 3 | 9 | 10000 | 10000 | 5000 |
| | 2006 | 0.6 | 35 | 2000 | 2000 | 200 |
| Tc | 2016 | 0.6 | 1.8 | 1000 | 1000 | 1000 |
| | 2006 | 0.1 | 0.2 | 5000 | 5000 | 5000 |
| Th | 2016 | 900 | 2000 | 10000 | 10000 | 2000 |
| | 2006 | 900 | 2000 | 5000 | 5000 | 500 |
| U | 2016 | 300 | 400 | 5000 | 5000 | 5000 |
| | 2006 | 200 | 300 | 5000 | 5000 | 5000 |
| Zr | 2016 | 900 | 2000 | 10000 | 10000 | 2000 |
| | 2006 | 900 | 2000 | 5000 | 5000 | 500 |

*Results*. Comparisons of flux to the water table for the nine parent radionuclides and daughters as calculated in the 2008 PA and in the current modeling approach are shown in Figure 6-19 through Figure 6-25. All radionuclide releases are $K_d$ controlled. The 2008 PA results were extracted from files for each radionuclide located in archival storage location:

\\gecko1\hpc_archive\pa\ArchiveHolding\Analysis\LAWV\PA\2008\Groundwater\vadose\transport\CrackedNoCdp\

Files used for each radionuclide were, for example, C-14\FluxWT_C-14.dat. The cracked concrete analysis without Cdp factors for carbonaceous material in the waste appears to be most like the current calculation. (Cdp factors were adjustments applied to Kd values in the 2008 PA for waste in a carbonaceous environment. They are not used in the present analysis.) Both Cracked and Uncracked 2008 PA results were examined and there was surprisingly little difference between the two. Comparison plots in this section of the report use the 2008 Cracked analysis.

2008 PA results for C-14, Cl-36 and I-129, shown in Figure 6-19 and Figure 6-20, all have the same general characteristics with three peaks in flux extending from a more gradual flux curve followed by another sharp peak at about 2000 years. These peaks occur at the same time for each radionuclide and, as annotated on the I-129 plot, occur when there is an increase in flow and when the LAWV roof collapses. Only eight infiltration flows were used in the 2008 PA modeling which likely caused the irregular flux shapes. The increases in $K_d$ shown in Table 6-4 also affect the results with all of the current flux peaks occurring later than in the 2008 PA calculations. The C-14 peak flux in the current model occurs beyond the compliance period (171 to 1171 years). Cl-36 also peaks outside of the compliance period while I-129 peaks just at the outer edge; however, allowing for transport time to the point of assessment, the peak I-129 flux will produce a maximum dose outside of the compliance period. The C-14 peak flux is approximately 50% of the 2008 PA value, the Cl-36 about the same as the 2008 PA result, and the I-129 peak over twice the 2008 PA value. The C-14 peak in the current model is increased by the roof collapse timing.

The peak current H-3 flux shown in Figure 6-20, which appears well before concrete degradation starts and before there is significant infiltration through the vault, is about 20% of the 2008 PA peak flux. The timing of the peak flux is in close agreement between the two models. Both peaks show a flux decrease when the closure cap is applied (171 years in the current model 125 years in the 2008 PA). Because there is little flow through the LAWV before and immediately after closure cap placement, the H-3 flux must be caused by diffusion out of the vault. The 2008 PA placed the waste at the midpoint of operations while the current simulation places the waste at the start of operations. The earlier placement adds about one half-life to the H-3 which would decrease the peak flux by a factor of two. In either case, fluxes to the water table from one gmol of H-3 are relatively small.

The large increase in $K_d$ for Nb-94 between 2008 ($K_d = 0$) and the current value ($K_d = 1000$) precludes a direct comparison of fluxes for this radionuclide as shown in Figure 6-21. However, the overall trend is correct with a much later flux peak in the current model using increased $K_d$. The later elution will likely remove Nb-94 from consideration for groundwater protection limits.

In both models, the peak Tc-99 fluxes shown in Figure 6-21 occur shortly after concrete $K_d$ values are replaced with soil $K_d$ values. This transition occurs at about 4700 years in the 2008 PA model and 3000 years in the current model. In addition to increased flow through the vault, the current model assumes $K_d$ values change from concrete to soil when the vault roof collapses while the 2008 PA model transition is based on 4000 pore-volume exchanges in the concrete.

In Figure 6-22, Figure 6-23 and Figure 6-24, results are plotted on both linear and semi-log scales to include daughter radionuclides which are at much lower levels than the parents. The Np-237 and U-235 series in Figure 6-22 and Figure 6-20, respectively, show similar behavior. As shown in Table 6-4, $K_d$ values for Np-237 in the latest chemical data package increased for sandy soil, decreased for clayey soil and increased for cement. Pa-231 $K_d$ values are identical to those of Np-237. The net effect is that current Np-237 and Pa-231 fluxes to the water table peak later than the 2008 PA fluxes and the peaks are sharper because they occur near the time of roof collapse. Uranium transport in both figures is very similar even though it is the parent radionuclide in one case and a decay product in the other. Uranium $K_d$ values in soil have increased in the latest chemical database causing peak fluxes to occur later in the current model. Examining the semi-log plots, there is a definite tendency in the current model for the fluxes to continue at a low level over a long time. The daughter radionuclides are decay products that follow the parent's behavior. This effect is also noticeable in the concentration profiles for C-14 in Appendix C where a small residual concentration of contaminant appears to remain in the vicinity of the vault walls after most of the material has been eluted.

Figure 6-24 shows flux to the water table for Zr-93 and its daughter Nb-93m. The linear plot of Zr-93 flux is distorted by the extreme difference in scale with the PA flux magnified by a factor of 5000 relative to the flux from the current model. As before, a direct comparison of Nb fluxes cannot be made because of the large difference in $K_d$. values between the two models. The semi-log plot appears to show that Zr-93 is behaving differently in the current model than in the 2008 PA version even though $K_d$ values have not changed. However, not capturing the peak flux for Zr-93 makes it difficult to compare the two calculations because the plot is only showing the leading edge of the peak.

Finally, Tc-99 and Np-237, which appeared to be potentially problematic, were replotted as shown in Figure 6-25 to examine the flux peaks more closely. The Tc-99 is just crossing the 2008 PA result at the end of the period of compliance and Np-237 flux curve falls below 2008 PA results except between about 3300 and 4300 years.

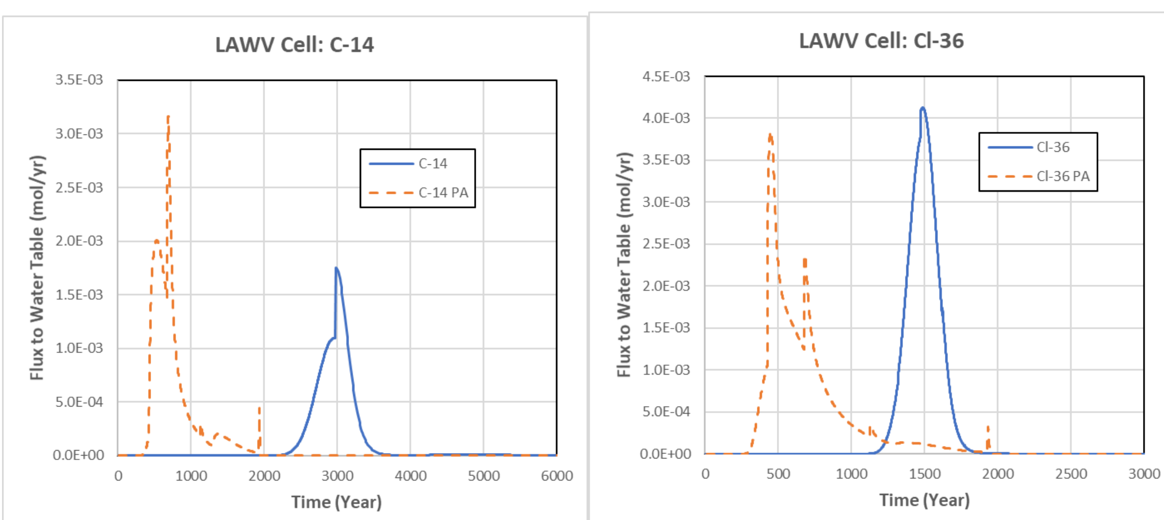


**Figure 6-19 Flux to water table for C-14 and Cl-36 in current and PA models.**

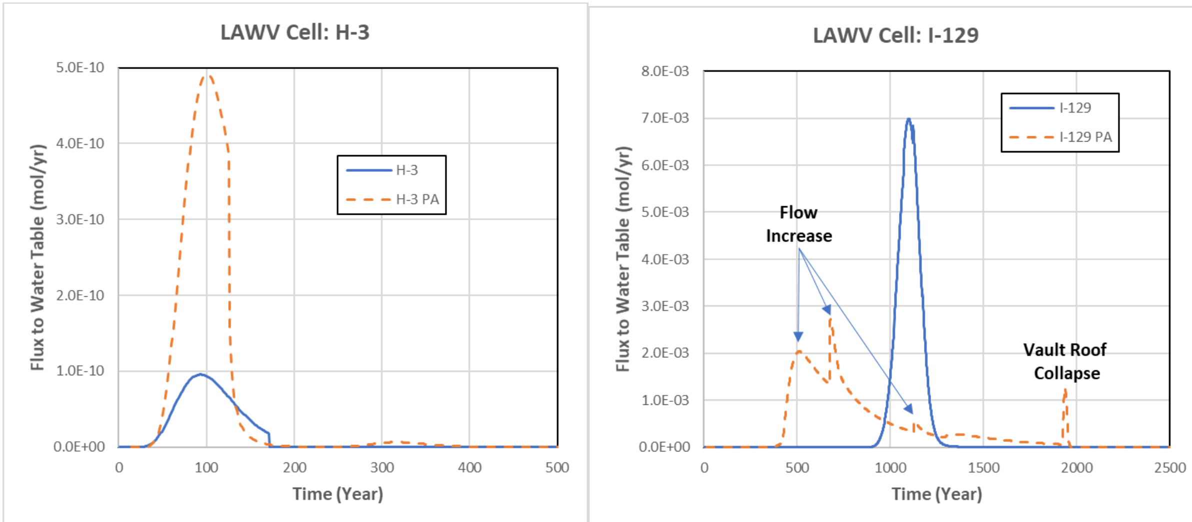


**Figure 6-20 Flux to water table for H-3 and I-129 in current and PA models.**

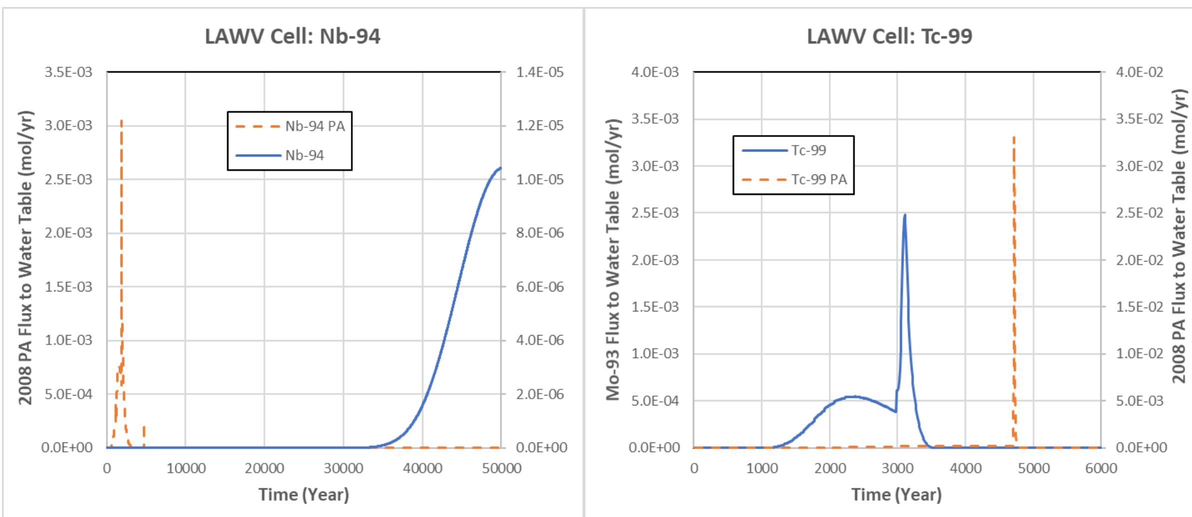


**Figure 6-21 Flux to water table for Nb-94 and Tc-99 in current and PA models.**

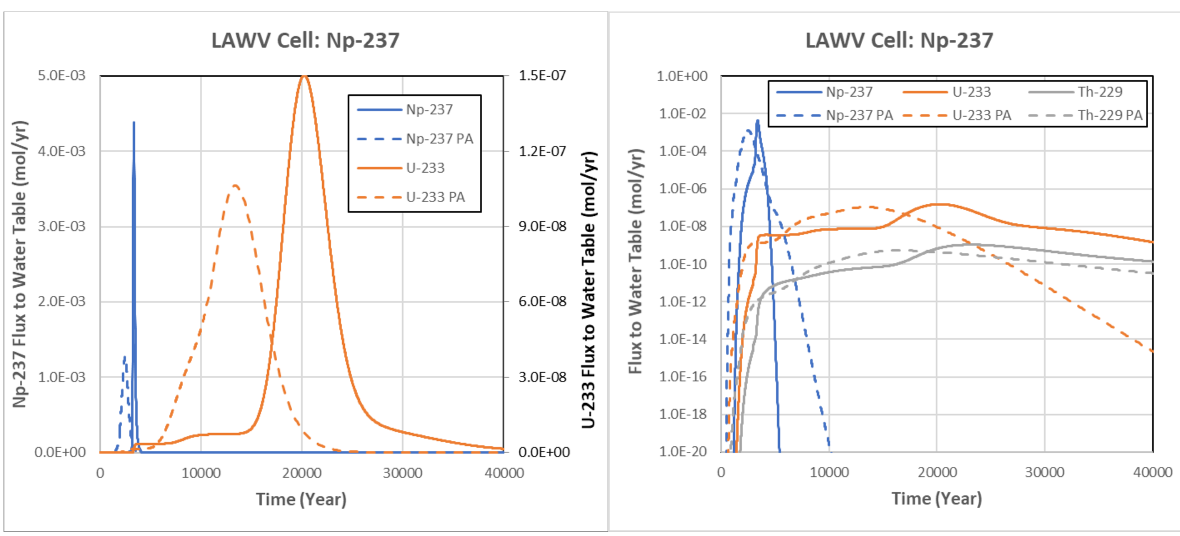


**Figure 6-22 Flux to water table for Np-237 and daughters in current and PA models.**

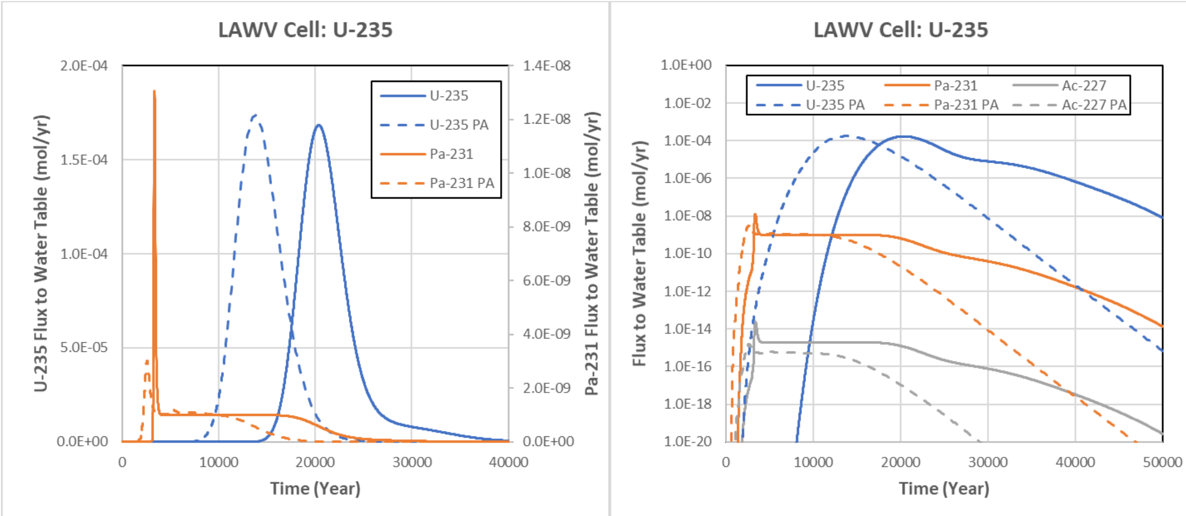


**Figure 6-23 Flux to water table for U-235 and daughters in current and PA models.**

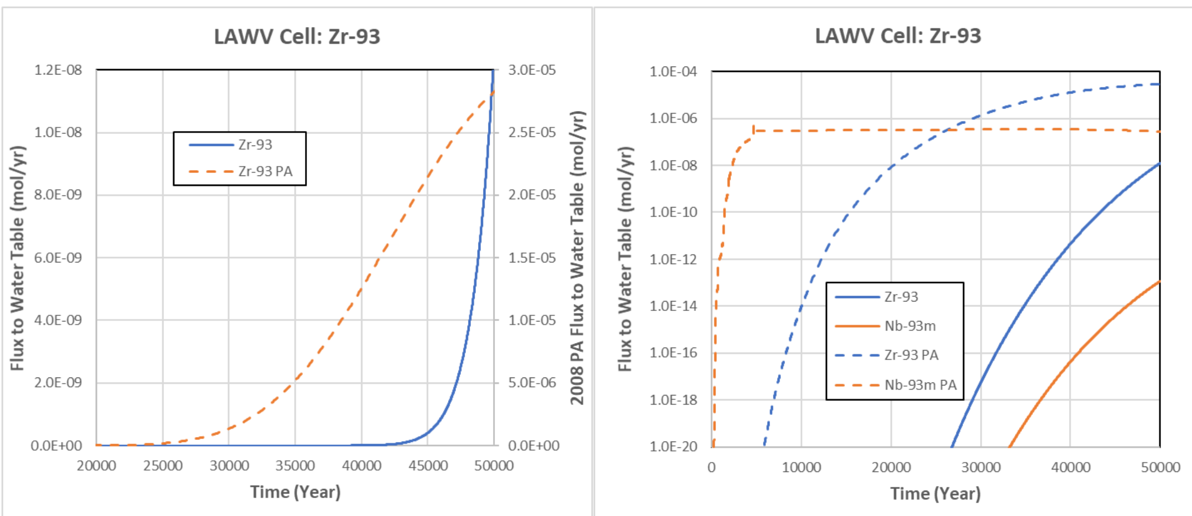


**Figure 6-24 Flux to water table for Zr-93 and Nb-93m in current and PA models.**

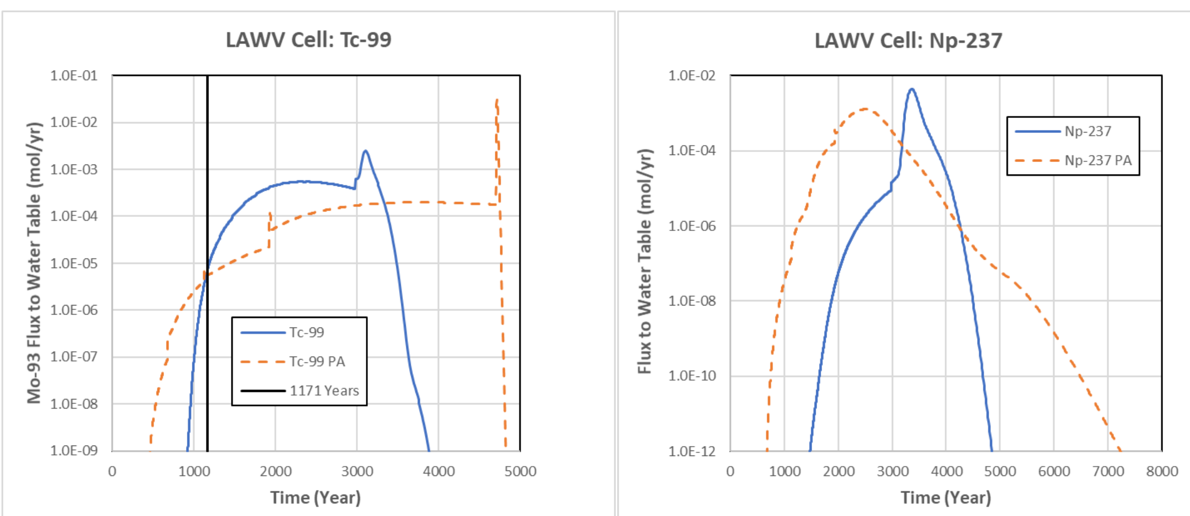


**Figure 6-25 Peak fluxes for Tc-99 and Np-237 in current and PA models.**

## 7.0 Conclusions

This report describes the development and testing of a new PORFLOW model to calculate water flow and radionuclide transport through the E-Area LAWV and its associated vadose zone. The model is geometrically similar to the one used for the 2008 E-Area PA. Improvements made to the previous model include:

- A refined computational mesh encompassing a larger area.
- Implementation of a different method to model cracking and degradation of concrete as it affects hydraulic properties.
- Including a drainage layer below the geomembrane in the model that more closely represents the HELP infiltration modeling.
- Updated vadose zone structure.
- Revised infiltration rates.
- Updated material properties.
- Updated solid-liquid distribution coefficients and solubilities.

Results for all flow calculations required to perform the next PA and for trial radionuclide transport calculations are shown in the report. As seen in Section 6.2.4, result of the transport calculations obtained with the model are significantly different than those obtained in 2008. The reasons for the difference can primarily be attributed to four factors:

1. Revised infiltration calculations.
2. Revised sorption properties.
3. The use of more time steps in the current calculation.
4. Different approaches to modeling concrete cracking and degradation.

All the radionuclide transport results obtained with the revised model appear to be reasonable and flux peaks to the water table generally occur further out in time than in the previous 2008 PA results. Nevertheless, not all radionuclides with LAWV limits have been tested and, in some cases, peak flux to the water table may exceed the 2008 values during the period of compliance causing disposal limits to decrease.

**8.0 References**

Bagwell, L.A., and P.L. Bennett, 2017. *Elevation of Water Table and Various Stratigraphic Surfaces Beneath E-Area Low Level Waste Disposal Facility*, SRNL-STI-2017-00301, Revision 1, November 2017.

C-CT-E-00084, 2016. *Preliminary E-Area Low Level Waste Facility (ELLWF) Conceptual Closure Cap – Details*, Sheet 1 of 4, Revision A, Savannah River Nuclear Solutions, Aiken, SC.

Carey, S. 2005. Low Activity Waste (LAW) Vault Structural Degradation Prediction, T-CLC-E-00018, Rev. 0. Westinghouse Savannah River Company, Aiken, South Carolina. October 27, 2005.

Cook, J. R., Phifer, M. A., Wilhite, E. L, Young, K. E., and Jones, W. E. 2004. *Closure Plan for the E-Area Low-Level Waste Facility*, Revision 4, WSRC-RP-2000-00425. Westinghouse Savannah River Company, Aiken, South Carolina. May 2004.

Dyer, J. A., 2019. *Infiltration Data Package for the E-Area Low-Level Waste Facility Performance Assessment*, SRNL-STI-2019-00363, Revision 0, November 2019.

Flach, G. P., 2017. *Method for Modeling the Gradual Physical Degradation of a Porous Material*, SRNL-STI-2017-00525, Revision 0, September 20, 2017.

Jones, W. E. and Phifer, M. A. 2006. E-Area Low-Activity Waste Vault Subsidence Potential and Closure Cap Performance (U), WSRC-TR-2005-00405. Westinghouse Savannah River Company, Aiken, South Carolina. September 2006.

Kaplan, D. I., 2016. *Geochemical Data Package for Performance Assessment Calculations Related to the Savannah River Site, SRNL-STI-2009-00473*, Revision 1, July 22, 2016.

McDowell-Boyer, L., Yu, A. D., Cook, J. R., Kocher, D. C., Wilhite, E. L., Holmes-Burns, H., and Young, K. E. 2000. *Radiological Performance Assessment for the E-Area Low-Level Waste Facility,* Revision 1, WSRC-RP-94-218. Westinghouse Savannah River Company, Aiken, South Carolina. January 31, 2000.

Nichols, R. L. and B. T. Butcher, 2020. *Hydraulic Properties Data Package for the E-Area Soils, Cementitious Materials, and Waste Zones – Update*, SRNL-STI-2019-00355, Revision 1, May 2020.

Phifer, M. A. and Wilhite, E. L. 2001. Waste Subsidence Potential versus Supercompaction. WSRC-RP-2001-00613, Westinghouse Savannah River Company, Aiken, South Carolina. October 5, 2001,

Phifer, M. A. and Nelson, E. A. 2003. *Saltstone, Disposal Facility Closure Cap Configuration and Degradation Base Case: Institutional Control to Pine Forest Scenario (U)*, Revision 0, WSRC-TR-2003-00436. Westinghouse Savannah River Company, Aiken, South Carolina, September 22, 2003.

Phifer, M. A., 2004. Preliminary E-Area Trench Closure Cap Closure Sequence, Infiltration, and Waste Thickness (U), WSRC-TR-2004-00119, Westinghouse Savannah River Company, Aiken, South Carolina. March 2004.

WSRC, 2008. *E-Area Low-Level Waste Facility DOE 435.1 Performance Assessment, Chapter 3 Low Activity Waste Vault,* WSRC-STI-2007-00306, Revision 0, July 2008.

## Appendix A Pressure Distribution in PORFLOW LAWV Model

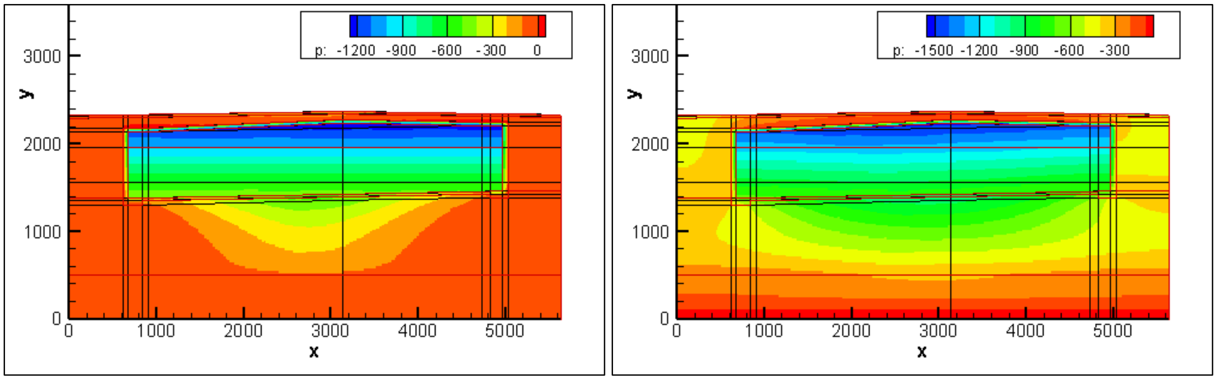


**Figure A-1 LAWV Suction Pressure for 0 – 171 and 171 – 221 years.**

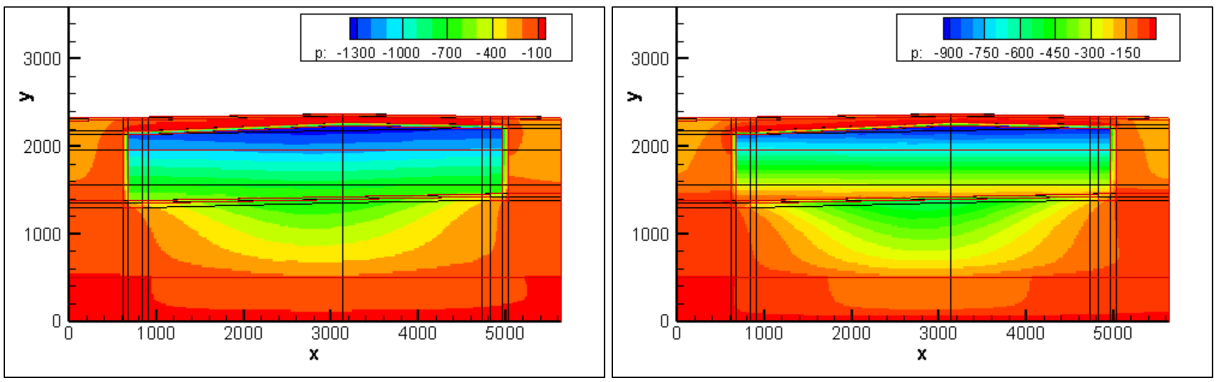


**Figure A-2 LAWV Suction Pressure for 221 – 271 and 271 – 321 years.**

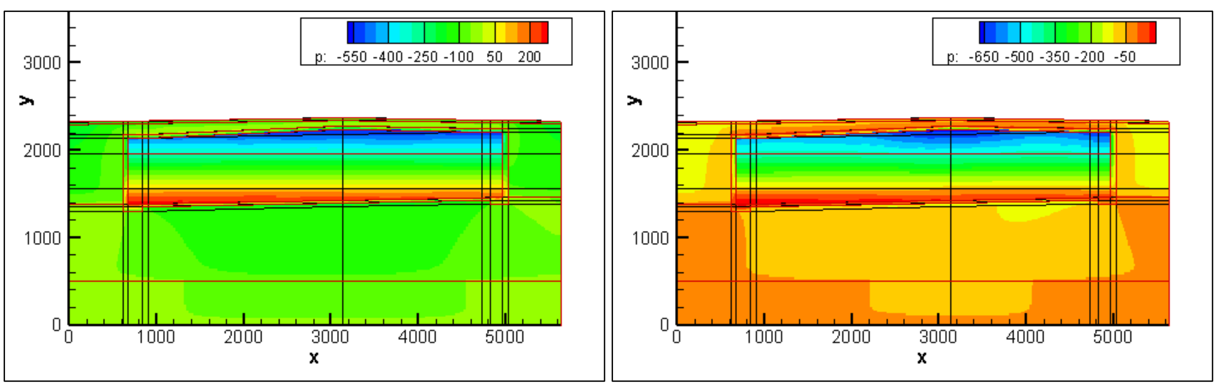


**Figure A-3 LAWV Suction Pressure for 321– 371 years and 371 – 421 years.**

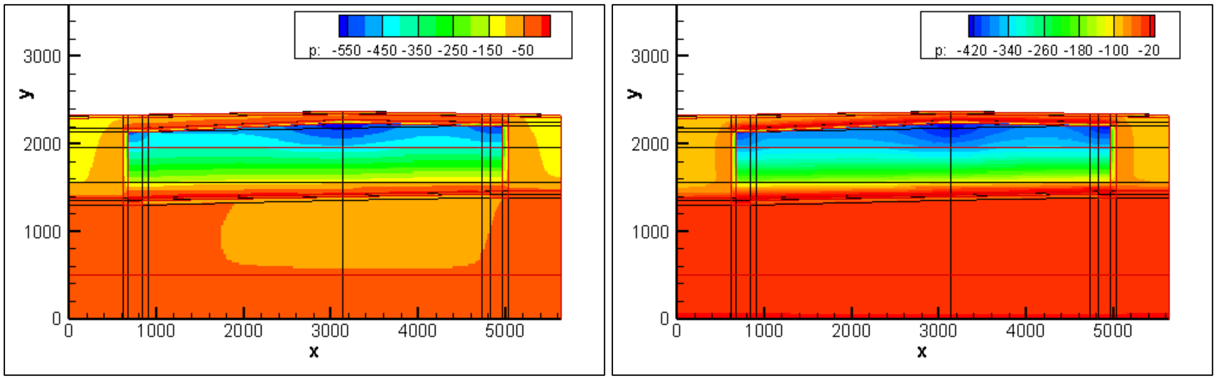


**Figure A-4 LAWV Suction Pressure for 421 – 471 years and 471 – 521 years.**

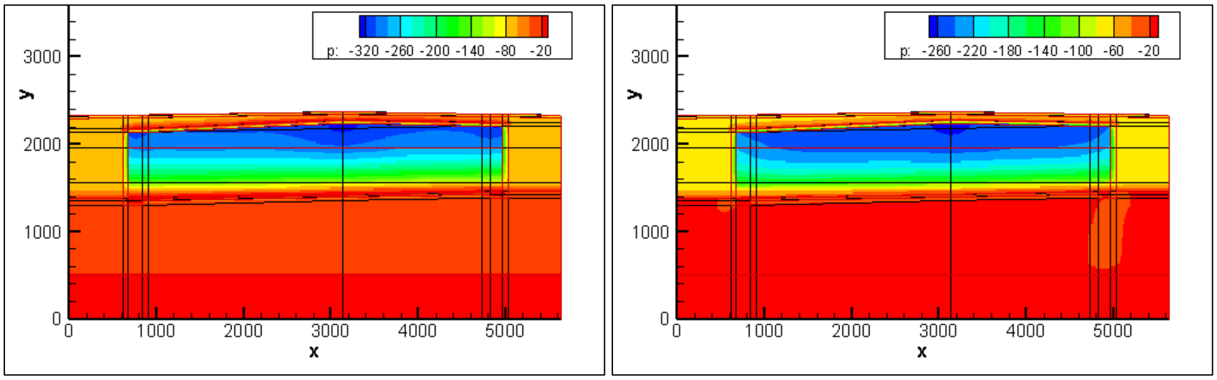


**Figure A-5 LAWV Suction Pressure for 521 – 571 years and 571 – 621 years.**

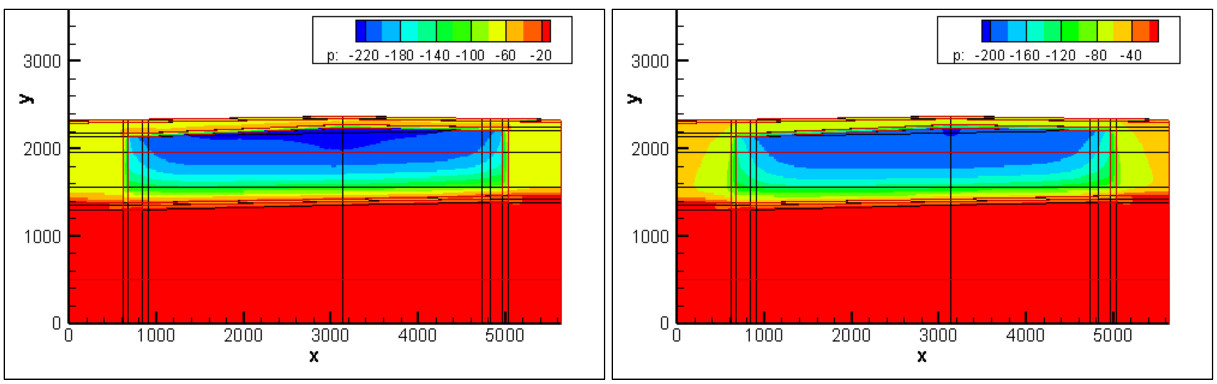


**Figure A-6 LAWV Suction Pressure for 611 – 671 years and 671 – 721 years.**

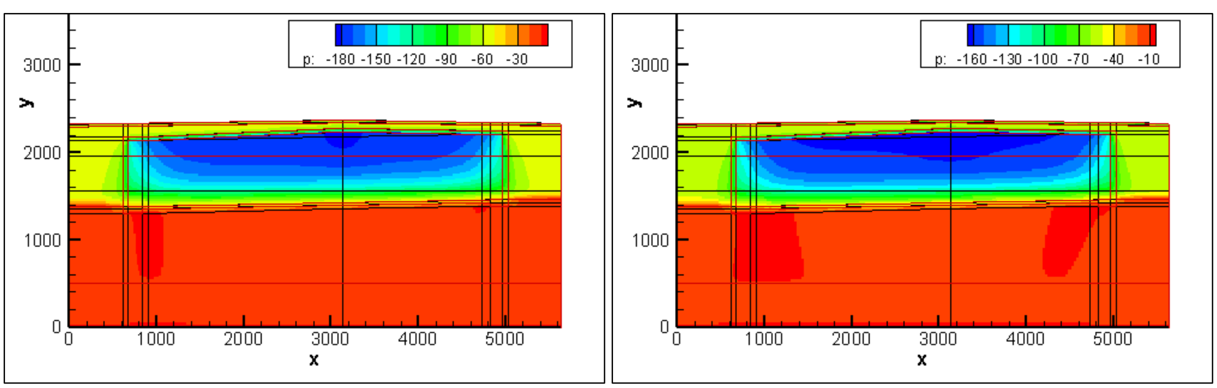


**Figure A-7 LAWV Suction Pressure for 721 – 771 years and 771 – 821 years.**

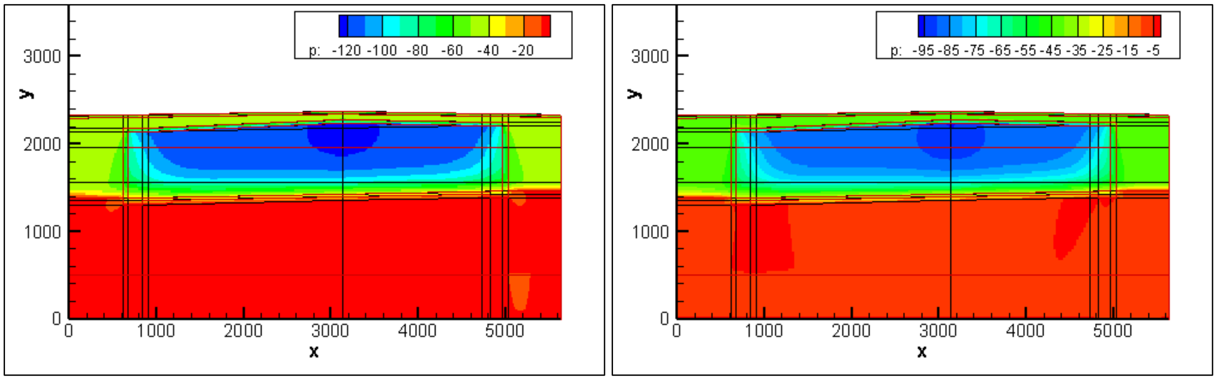


**Figure A-8 LAWV Suction Pressure for 971 – 1021 years and 1171 – 1321 years.**

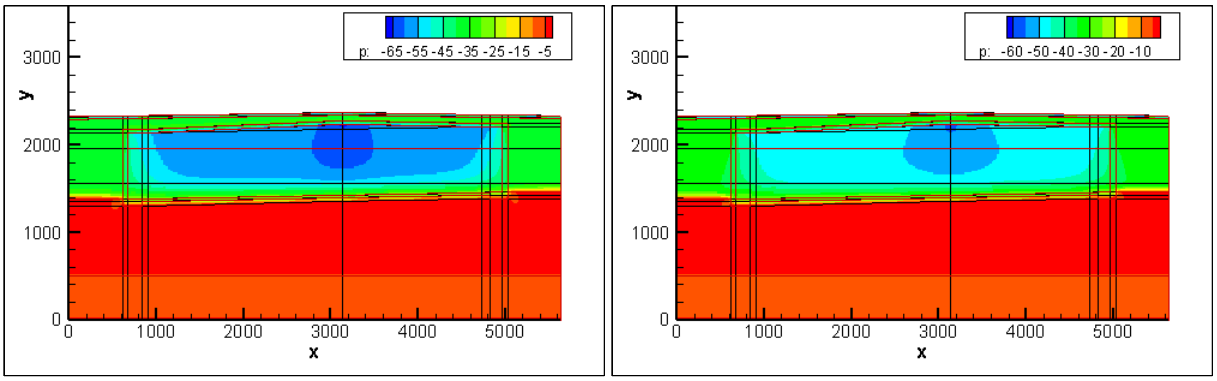


**Figure A-9 LAWV Suction Pressure for 1771 – 1921 years and 2371– 2521 years.**

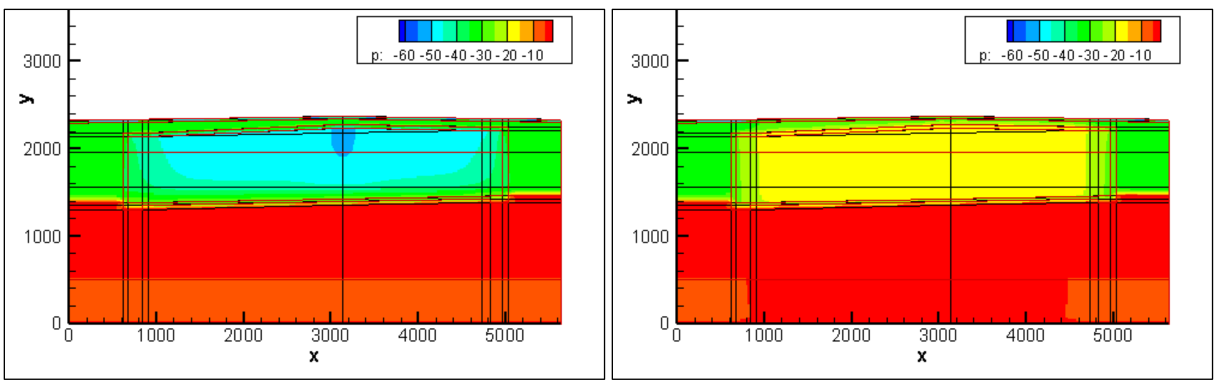


**Figure A-10 LAWV Suction Pressure for 2821 – 2976 years and >2976 years.**

# Appendix B Water Saturation in PORFLOW LAWV Model

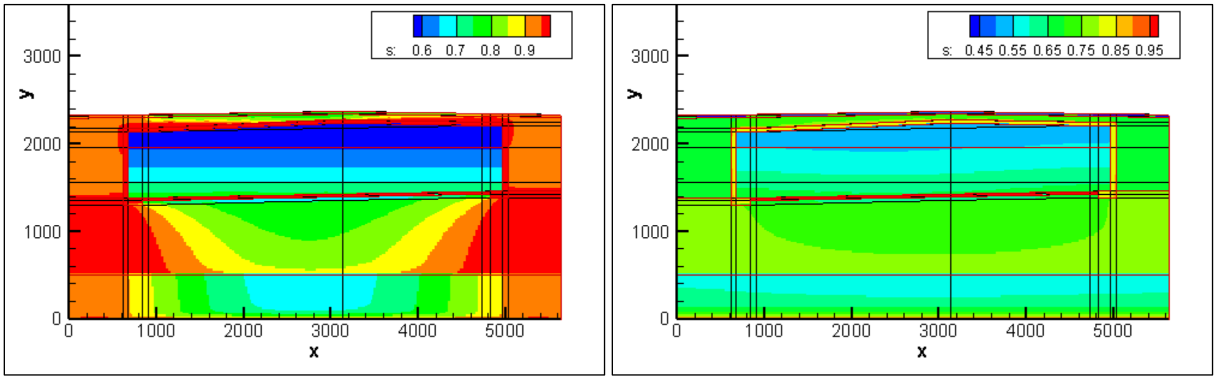


**Figure B-1 LAWV Water Saturation for 0 – 171 and 171 – 221 years.**

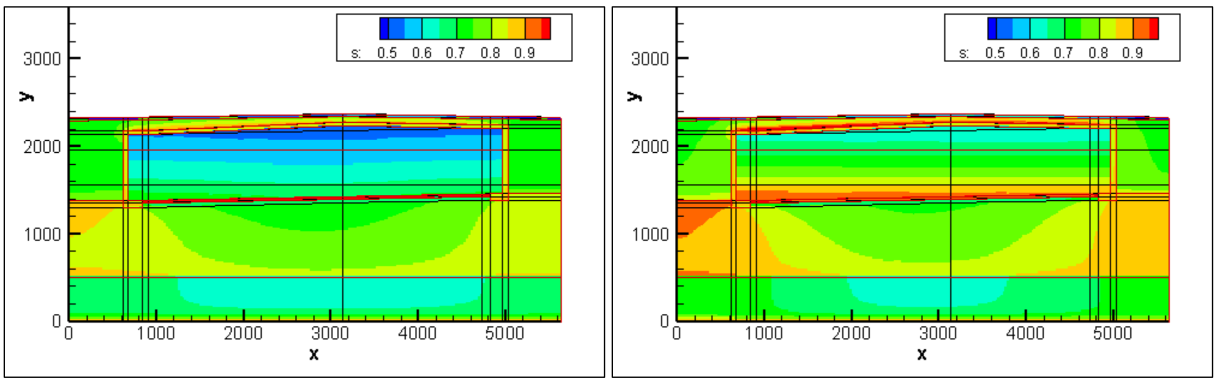


**Figure B-2 LAWV Water Saturation for 221 – 271 and 271 – 321 years.**

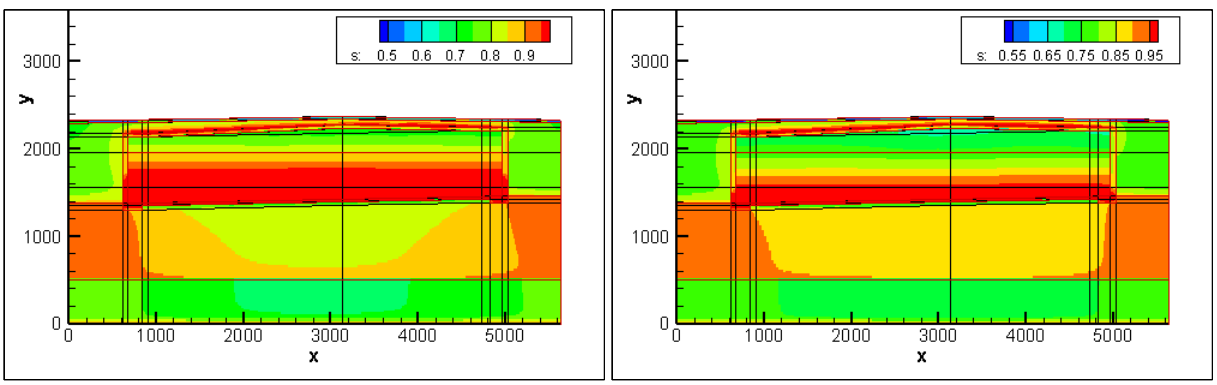


**Figure B-3 LAWV Water Saturation for 321– 371 years and 371 – 421 years.**

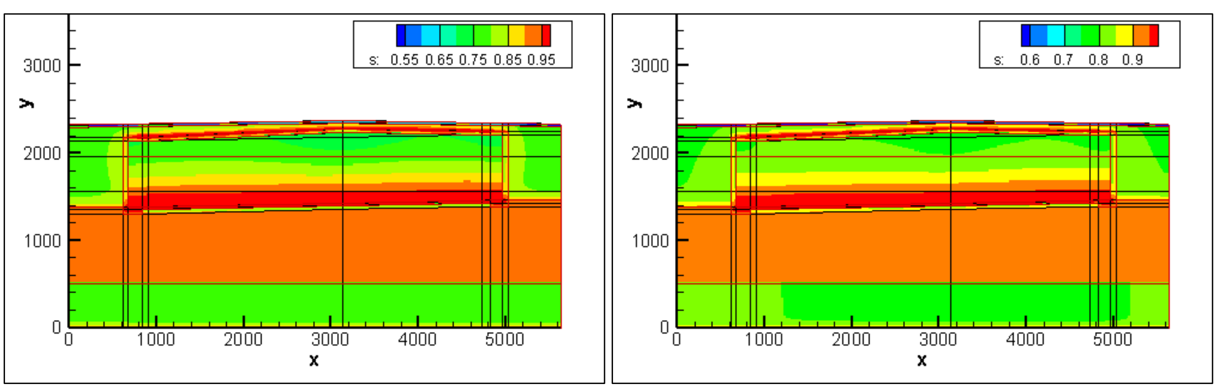


**Figure B-4 LAWV Water Saturation for 421 – 471 years and 471 – 521 years.**

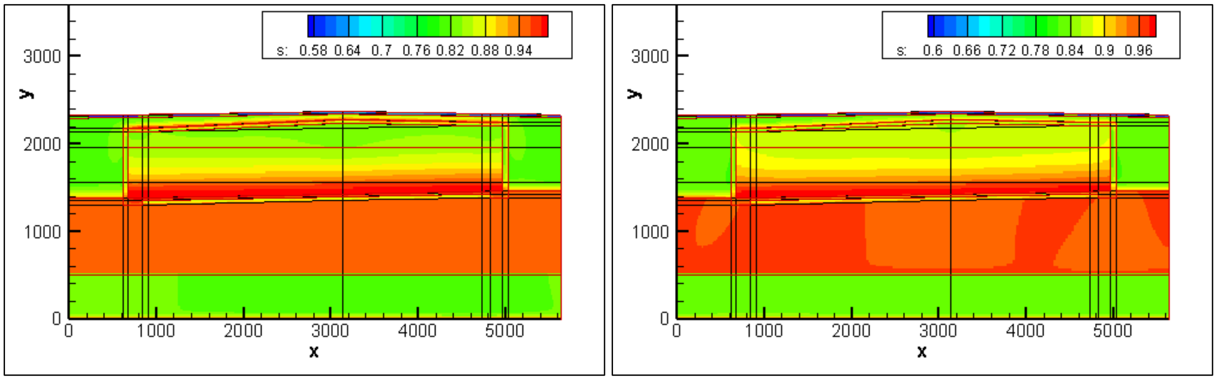


Figure B-5 LAWV Water Saturation for 521 – 571 years and 571 – 621 years.

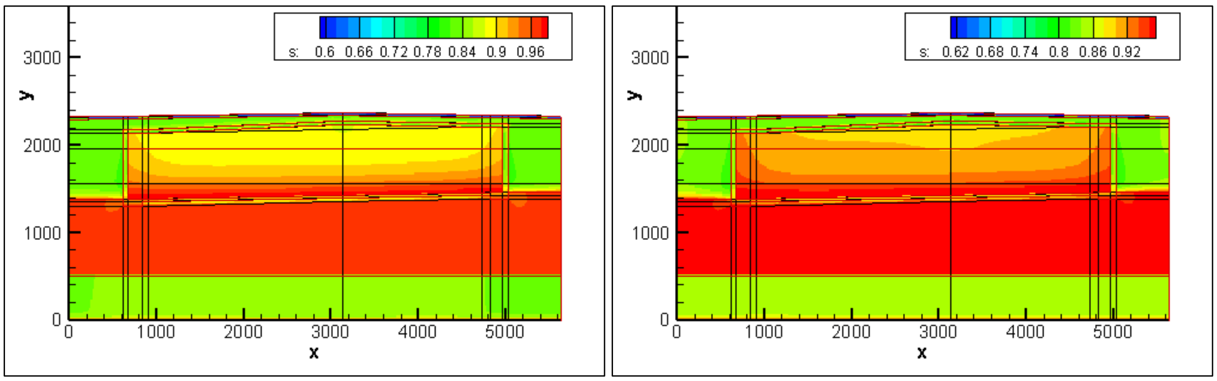


Figure B-6 LAWV Water Saturation for 611 – 671 years and 671 – 721 years.

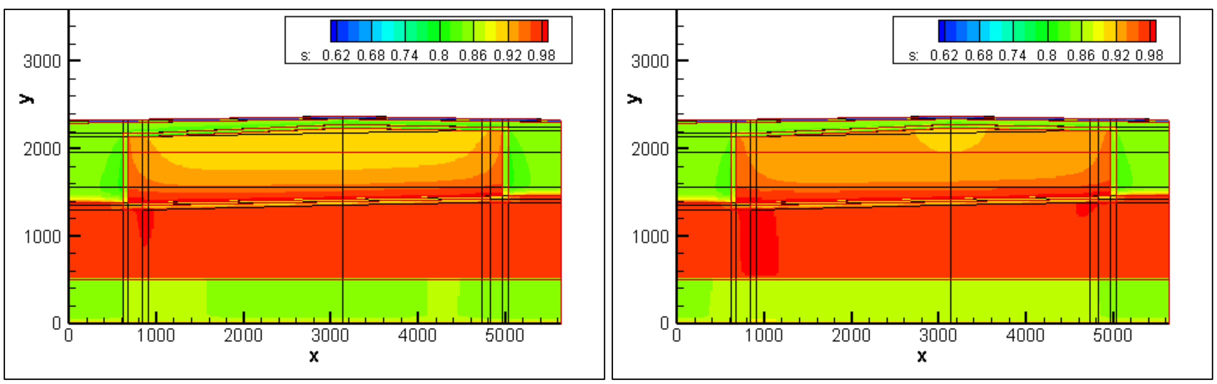


Figure B-7 LAWV Water Saturation for 721 – 771 years and 771 – 821 years.

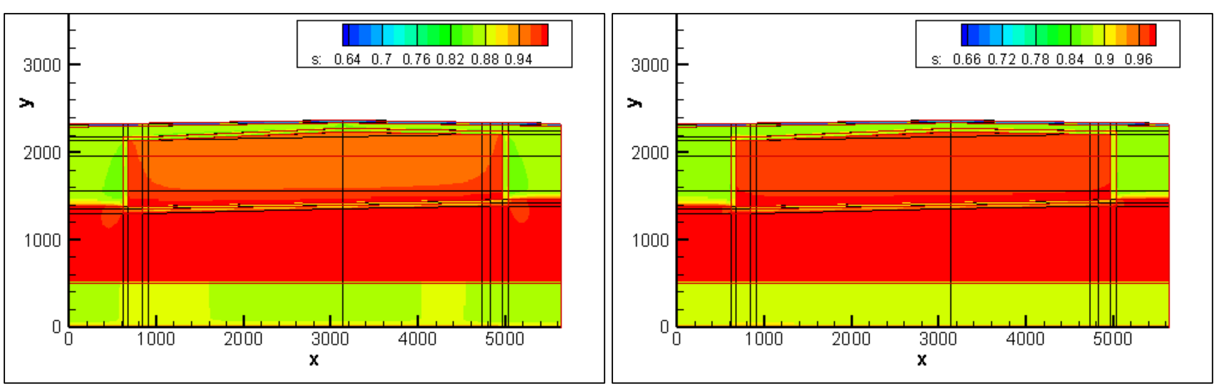


Figure B-8 LAWV Water Saturation for 971 – 1021 years and 1171 – 1321 years.

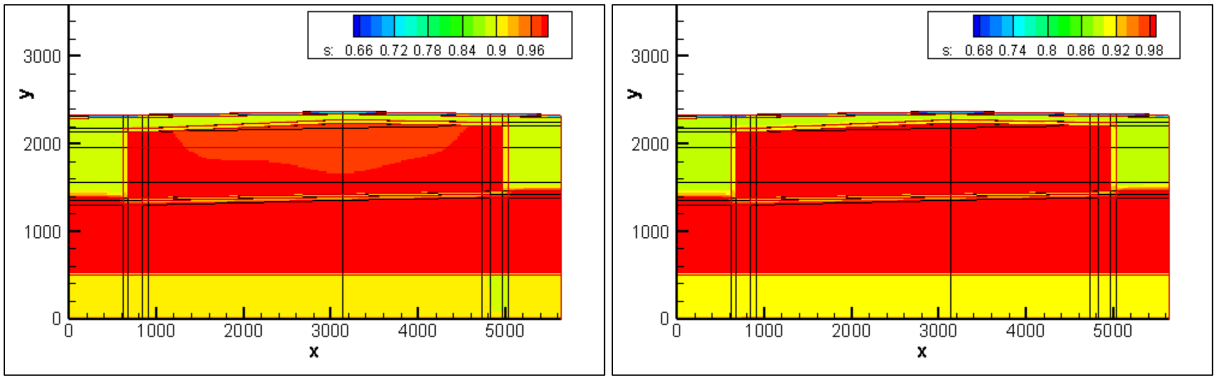


**Figure B-9 LAWV Water Saturation for 1771 – 1921 years and 2371– 2521 years.**

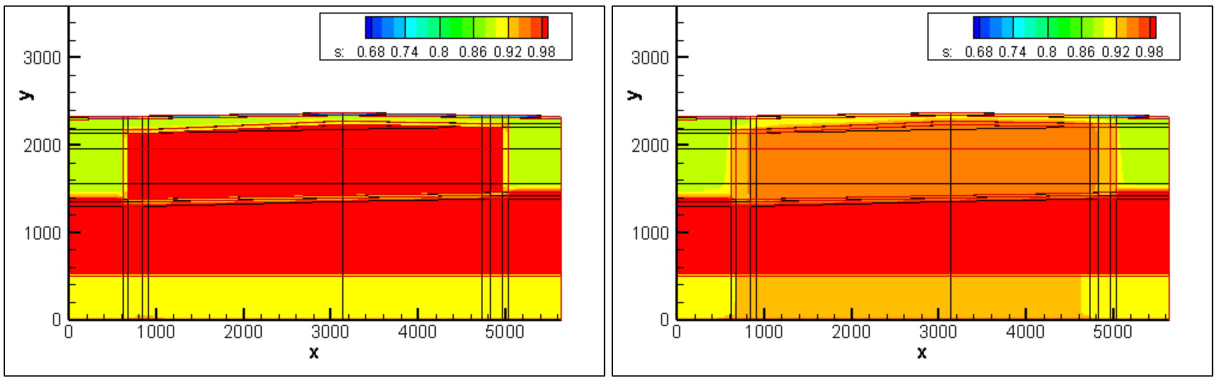


**Figure B-10 LAWV Water Saturation for 2821 – 2976 years and >2976 years.**

## Appendix C C-14 Concentration Profiles in LAWV Model

The concentration plots shown below follow C-14 elution from the LAWV from 50 to 6,000 years after the start of operations. Figure C-1 shows that C-14 has diffused up into the space above the waste deposition region during the initial period of low water infiltration. This space was given the properties of LAWV waste because of its high porosity. As shown in Figure C-2, by 750 years, the space above the waste has been effectively cleared of C-14 as infiltration increases and C-14 starts eluting into the upper vadose zone. Figure C-3 shows that it takes between 1500 and 2000 years for any measurable amount of C-14 to reach the water table. Figure C-4 shows the time period when C-14 concentrations at the water table are at their highest level. Collapse of the vault roof at about 3000 years increases infiltration through the vault region and the rate of vadose zone transport. The last two figures show that some small residual C-14 remains in the vicinity of the vault walls and in the vadose zone below the walls after the bulk of the C-14 has been transported out of the vadose zone.

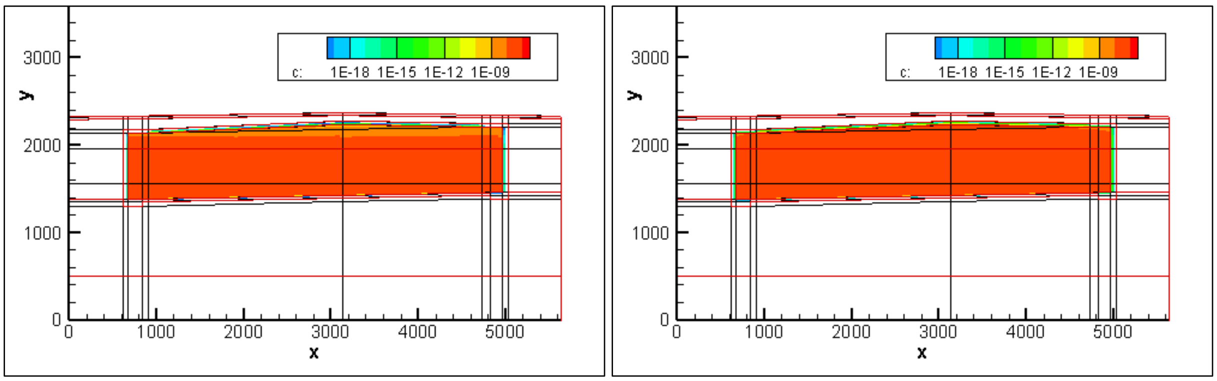


**Figure C-1 C-14 Concentration profiles at 50 and 250 years.**

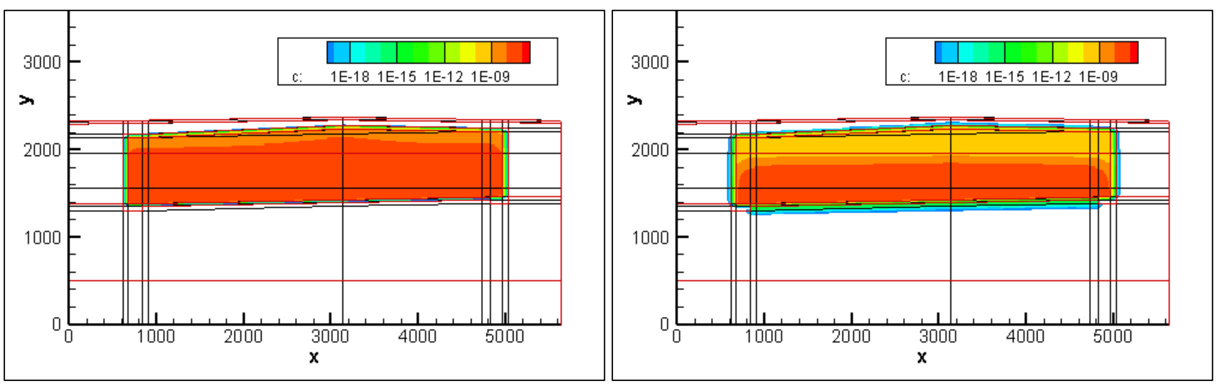


**Figure C-2 C-14 Concentration profiles at 500 and 750 years.**

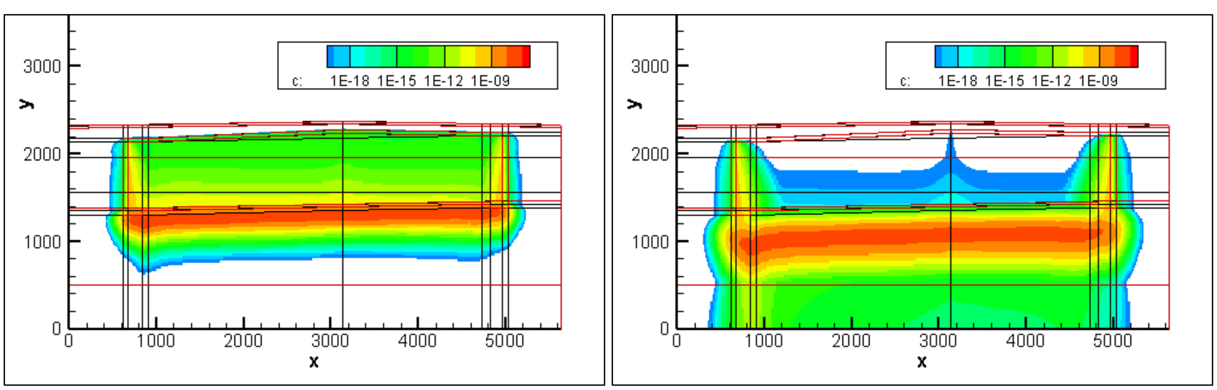


**Figure C-3 C-14 Concentration profiles at 1500 and 2000 years.**

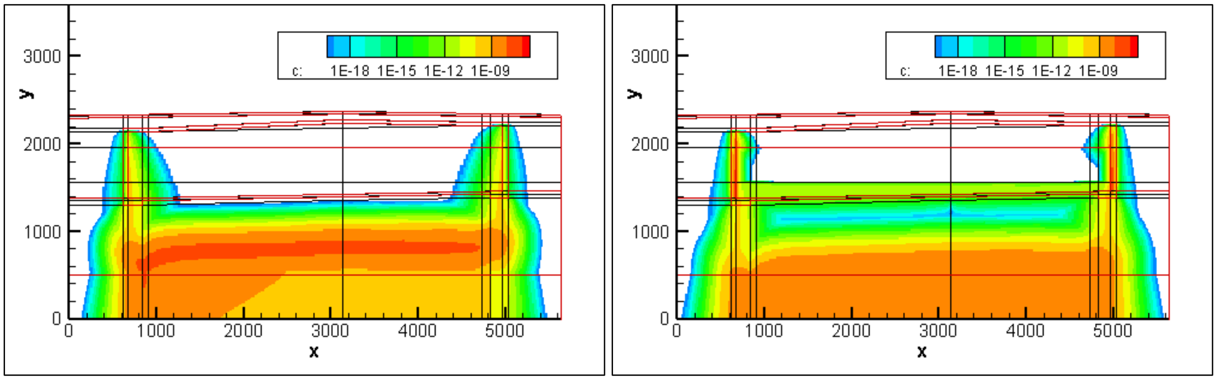


**Figure C-4 C-14 Concentration profiles at 2500 and 3000 years.**

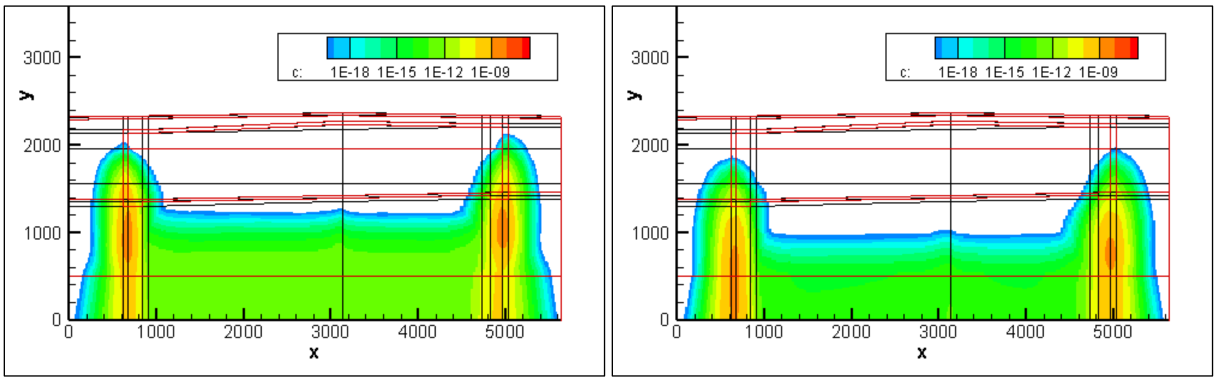


**Figure C-5 C-14 Concentration profiles at 4000 and 4500 years.**

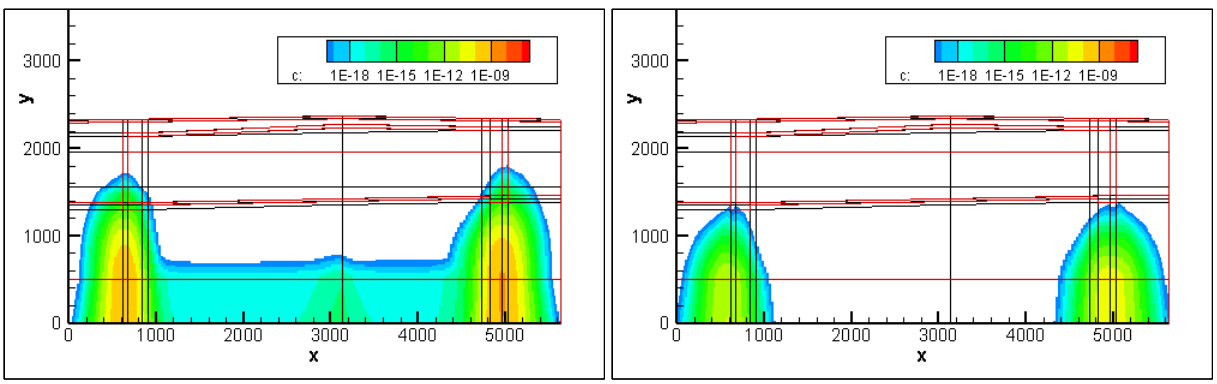


**Figure C-6 C-14 Concentration profiles at 5000 and 6000 years.**

**Distribution:**

cj.bannochie@srnl.doe.gov
alex.cozzi@srnl.doe.gov
a.fellinger@srnl.doe.gov
samuel.fink@srnl.doe.gov
brenda.garcia-diaz@srnl.doe.gov
connie.herman@srnl.doe.gov
dennis.jackson@srnl.doe.gov
brady.lee@srnl.doe.gov
patricia.lee@srnl.doe.gov
joseph.manna@srnl.doe.gov
daniel.mccabe@srnl.doe.gov
gregg.morgan@srnl.doe.gov
frank.pennebaker@srnl.doe.gov
william.ramsey@srnl.doe.gov
eric.skidmore@srnl.doe.gov
michael.stone@srnl.doe.gov
boyd.wiedenman@srnl.doe.gov
terry.foster@srnl.doe.gov

Records Administration (EDWS)

sebastian.aleman@srnl.doe.gov
diana.bowers@srs.gov
tom.butcher@srnl.doe.gov
kerri.crawford@srs.gov
thomas.danielson@srnl.doe.gov
kenneth.dixon@srnl.doe.gov
james.dyer@srnl.doe.gov
peter.fairchild@srs.gov
maximilian.gorensek@srnl.doe.gov
luther.hamm@srnl.doe.gov
thong.hang@srnl.doe.gov
daniel.kaplan@srnl.doe.gov
elizabeth.labone@srnl.doe.gov
dien.li@srs.gov
steven.mentrup@srs.gov
verne.mooneyhan@srs.gov
ralph.nichols@srnl.doe.gov
virginia.rigsby@srs.gov
jansen.simmons@srs.gov
frank.smith@srnl.doe.gov
ira.stewart@srs.gov
jennifer.wohlwend@srnl.doe.gov